

Durham E-Theses

*The roles of the RPD3 histone deacetylase in
facilitating transcriptional responses to osmotic stress
in S. cerevisiae*

NELSON, JOSEPH,FRANCIS

How to cite:

NELSON, JOSEPH,FRANCIS (2017) *The roles of the RPD3 histone deacetylase in facilitating transcriptional responses to osmotic stress in S. cerevisiae*, Durham theses, Durham University. Available at Durham E-Theses Online: <http://etheses.dur.ac.uk/12358/>

Use policy

The full-text may be used and/or reproduced, and given to third parties in any format or medium, without prior permission or charge, for personal research or study, educational, or not-for-profit purposes provided that:

- a full bibliographic reference is made to the original source
- a [link](#) is made to the metadata record in Durham E-Theses
- the full-text is not changed in any way

The full-text must not be sold in any format or medium without the formal permission of the copyright holders.

Please consult the [full Durham E-Theses policy](#) for further details.

**The roles of the *RPD3* histone
deacetylase in transcriptional responses
to osmotic stress in *S. cerevisiae***

Joseph Francis Nelson

Submitted for the degree of Master of Science in
the Department of Biosciences

Durham University

March 2017

ABSTRACT

Modification of N-terminal histone tails is one of the major mechanisms by which chromatin state is modified to influence transcription, alongside DNA methylation. The most widely observed of the various histone modifications is acetylation, which is canonically known as a transcriptional up regulator. However, this view has been challenged by observations that *RPD3*, a widely-conserved histone deacetylase in *S. cerevisiae*, is required for full transcriptional induction during various stress responses in this organism. *RPD3* forms 3 protein complexes in the cell known as Rpd3L, Rpd3S and Rpd3 μ and it has not been defined in the literature which of these complexes mediates *RPD3* action during the osmotic stress response. Furthermore, the mechanism by which *RPD3* mediates transcriptional activation is undefined, with conflicting results in the literature. In this research, northern blotting analysis is carried out to analyse the transcriptional responses of strains carrying deletions in subunits of different *RPD3* complexes to induction of osmotic stress via NaCl and sorbitol. Strains carrying deletions in Rpd3L subunits are found to be defective in the transcriptional response to osmotic stress, a result consistent with literature studies of other stress responses. CHIP-qPCR analysis is also carried out to analyse how histone acetylation is affected by osmotic stress, and how this is affected by loss of *RPD3* and members of the different *RPD3* complexes. Acetylation is found to increase at stress responsive loci after osmotic stress, alongside a depletion in total nucleosome occupancy. This is found to be decreased in strains carrying deletions in Rpd3L subunits, but not in strains carrying deletions in Rpd3S or Rpd3 μ strains. Overall, the data support a conclusion that *RPD3* mediates transcription via histone acetylation and nucleosome depletion at stress-responsive loci in response to osmotic stress, and that the Rpd3L complex is required for *RPD3* action in this stress response.

Declaration and statement of copyright

I declare that the composition of this thesis, and all data presented herein, is the result of my own work. No part of the material offered has previously been submitted for a higher degree.

“The copyright of this thesis rests with the author. No quotation from it should be published without the author's prior written consent and information derived from it should be acknowledged.”

Table of Contents

Abstract.....	2
Declaration and statement of copyright.....	3
Chapter 1 – Introduction.....	7
1.1 Review of Histone Modifications and Chromatin structure.....	7
1.1.1 Histones and Chromatin Structure.....	7
1.1.2 Histone Acetylation.....	10
1.2 The <i>S. cerevisiae</i> osmotic stress response.....	11
1.3 The <i>RPD3</i> Histone Deacetylase.....	13
1.3.1 Canonical and Recent Roles of <i>RPD3</i>	13
1.3.3 Regulation of <i>RPD3</i> Activity.....	18
1.4 Experimental Hypotheses and Objectives.....	22
Chapter 2 – Materials and Methods.....	26
2.1 Reagents and Chemicals.....	26
2.1 Culturing of Yeast Strains.....	29
2.2.1 Strains Utilised in this Study.....	29
2.2.2 Storage and Culturing of Yeast Strains.....	30
2.3 PCR-Mediated Gene Deletion.....	32
2.4 Northern Blotting.....	38

2.4.1 RNA Extraction and Blotting Procedure.....	38
2.4.2 Hybridisation of Membranes.....	39
2.4.3 Radioactive labelling of DNA probes.....	40
2.5 Chromatin Immunoprecipitation – quantitative PCR (ChIP-qPCR).....	41
2.5.1 Chromatin Cross-Linking and Immunoprecipitation.....	41
2.5.2 Quantitative PCR (qPCR).....	44
2.5.3 Analysis and Normalisation of ChIP-qPCR Data.....	45
Chapter 3 – Requirement for Rpd3L and Rpd3S complexes in transcriptional responses to osmotic stress.....	45
3.1 rpd3LΔ mutants show defect in the transcriptional response to NaCl-induced osmotic stress.....	47
3.2 No evidence of a defect in transcriptional responses to NaCl- induced osmotic stress was found in rpd3SΔ strains.....	53
3.3 Investigation of sorbitol stress responses and optimisation of stressing conditions.....	57
3.4 Summary and Discussion of Northern Blotting analysis.....	61
Chapter 4 - ChIP-qPCR Analysis of histone acetylation and occupancy during the osmotic stress response.....	64

4.1 rpd3LΔ strains display defect in acetylation and histone loss at stress-induced loci after osmotic stress.....	65
4.2 rpd3Δ strains show general decrease in acetylation after osmotic stress, whilst rpd3SΔ strains show a heightened level of acetylation.....	71
4.3 rpd3μΔ strains show acetylation at H3K9 and H4K8 during the osmotic stress response.....	
4.4 Summary and discussion of ChIP-qPCR analysis.....	75
Chapter 5 – General discussion and priorities for further work.....	79
5.1 rpd3LΔ strains display a general defect in transcriptional responses to osmotic stress.....	79
5.2 Histone acetylation and nucleosome loss is observed during the osmotic stress response, and a defect is observed in rpd3LΔ strains.....	81
5.3 Summary of data and potential hypotheses.....	83
5.4 Priorities for further work in this area.....	84
Chapter 6 – Bibliography.....	87

Chapter 1 – Introduction

1.1 Review of Histone Modifications and Chromatin

1.1.1 Histones and Chromatin Structure

DNA is not found as naked molecules inside eukaryotic cell nuclei. Instead, it exists in a complex with a variety of proteins, known as chromatin, which shows high conservation across the eukaryotic domain. The predominant proteins in this complex are the histone proteins Histone 1 (H1), Histone 2A (H2A), Histone 2B (H2B), Histone 3 (H3) and Histone 4 (H4). The basic repeating unit of chromatin is the nucleosome, which consists of 147 bp of DNA wrapped around an octamer of histones, formed by two H2A-H2B dimers and two H3-H4 dimers (Rando and Chang, 2009). Thus, these histones are known as the “core” histones, whilst H1 is referred to as the “linker” histone and has roles in organising the folding of strands of DNA between nucleosomes. The repeating nucleosome pattern creates a DNA fibre structure with a width of 10nm, often known as the “beads-on-a-string” form of DNA. This 10 nm fiber is now widely accepted as the predominant form in which DNA is found, at least in transcriptionally active genome locations (Fussner et al., 2011).

The widely-conserved chromatin structures found in eukaryotic nuclei are known to have several crucial roles in the cell. These include protection of the DNA molecule from stresses, maintaining chromosome integrity during cell division, and modulation of gene expression. Over the last 20 years, our knowledge of this latter role has hugely expanded, and it has come to be understood to represent one of the most complex areas of genetics. Correspondingly the relationship between chromatin structure and

gene expression has become an intense area of active research. One of the major mechanisms by which chromatin structure, and thus gene expression, are modified is via post-translational modifications of the core histones. A key feature of the nucleosome structure is that the N-terminal tails of these histones protrude from the nucleosome structure, allowing interaction with the surrounding environment. These tails are highly susceptible to a plethora of post-translational modifications, with at least nine identified to date (Bannister & Kouzarides, 2011).

As with most aspects of chromatin structure, as our understanding of histone modifications has grown, so has our appreciation of its complexity. Previously, the relationship between histones and transcriptions was thought to be relatively straightforward, with certain modifications activating transcription by disrupting interactions between nucleosomes and thus opening up the chromatin structure (Sternglanz, 1996, Pazin and Kadonaga, 1997). Meanwhile, others were thought to repress transcription by allowing tighter packaging of nucleosomes and formation of higher order chromatin structures. This view of how histone modifications affect chromatin state and gene expression is illustrated for acetylation (the modification that shall be examined in this study) in Figure 1 (reproduced from Pazin and Kadonaga, 1997). However, as aforementioned our current understanding of histone modifications is far more complex, with numerous features observed to challenge this linear view. Rather than some modifications always activating transcription and vice versa, it is now understood that the same modification can have different or even opposite effects depending upon the amino acid residue on which it occurs. For

Acetylation Induces a Conformational Change in the Core Histones



REPPRESSED

EXAMPLE

Lysine-rich tails bind tightly to DNA and repress transcription by blocking access of factors to the DNA template.



ACTIVE/COMPETENT

Acetylation of lysine residues alters chromatin structure and allows binding of transcription factors.

Figure 1 – Reproduced from Fig. 2, Pazin and Kadonaga, 1997.

Illustration of how acetylation affects nucleosome packaging, and correspondingly chromatin condensation. This mechanism was first proposed in 1998 and is now widely accepted in the field. It is now also known that acetylation can affect chromatin condensation indirectly through acting as a recruitment signal for other chromatin modifying enzymes

example, trimethylation of Histone 3 at lysine 4 (H3K4Me3) is known to activate transcription, whilst the same modification (trimethylation) at lysine 27 on H3 (H3K27Me3) is generally repressive (Berger, 2007). Equally, the same modification occurring at the same amino acid residue can have differing functionality depending on where within a gene it occurs. For example, increases of the modification H3K9Ac near the promoters of stress-responsive genes has been cited as important in activating transcriptional responses to osmotic stress in *S. cerevisiae*, whilst increasing this modification elsewhere in the gene body has little effect (Magraner-Pardo et al., 2014).

Finally, it is now understood that mechanisms by which modifications influence transcription may be far more complex than the direct methods first identified. Certain modifications also have “indirect” effects via facilitating other histone modifications or acting as a recruitment signal for other chromatin proteins (Berger et al., 2007, Bannister and Kouzarides, 2011). Histone acetylation is now known to have particularly marked indirect effects on gene expression via recruitment of other bromodomain-containing chromatin modifiers (reviewed in Josling et al., 2012). This particularly complicates studies in the area, as cross-talk between different modifications becomes possible, and modifications may not show a direct temporal correlation with the transcriptional responses they modulate.

1.1.2 Histone Acetylation

Of the various known histone modifications, acetylation is both the most widely observed and the best studied (Sternglanz, 1996). Two groups of enzymes control the prevalence of histone acetylation; histone acetyl transferases (HATs) add acetyl groups to histones and histone deacetylases (HDACs) remove them. As previously described for histone modifications in general a straightforward, simplified, view of histone acetylation was previously taken in the field. By the mid-1990s, a consensus had emerged that histone acetylation facilitated active gene expression, whilst deacetylation was repressive (Pazin and Kadonaga, 1997, Pennisi, 1997, Sternglanz, 1996). A linear view was also taken of the mechanism by which this occurred, with acetyl groups thought to disrupt contacts between histones and DNA, thus inhibiting tight packing of nucleosomes, as illustrated in Figure 1 (Reproduced from Pazin and Kagonga, 1997).

This mechanism is now widely accepted, although we now understand that acetylation can also have indirect effects on chromatin structure via recruitment of other chromatin-modifying enzymes. However, whilst most observations show a correlation between histone acetylation and gene activity, the correlation observed is not perfect. As with chromatin modifications in general, observations in the literature have challenged the previously accepted view, with numerous findings citing requirements for either deacetylation or deacetylase enzymes in activating transcription (Vidal and Gaber, 1991, Pazin and Kadonaga, 1997, De Nadal et al., 2004). Residue-specific and loci-specific effects of histone acetylation in transcriptional activation have also more recently been cited (Magraner-Pardo et al., 2014). Thus, histone acetylation ideally illustrates our modern appreciation of the complexity of chromatin, and transcriptional regulation. It also offers a warning against over-concluding or making simplifying assumptions in the area. The wealth of literature available for this modification also makes it an ideal target for further studies into the underlying mechanisms and unelucidated features of how histone modifications govern transcription.

1.2. The *S. cerevisiae* osmotic stress response

S. cerevisiae is a classic genetic model which has often been used to study the dynamics of histone modifications and how they modulate transcription in many situations. It is widely used as a model to study a variety of cellular processes due to its good suitability for lab work, with a short generation time (~90 mins in ideal conditions), an available reference genome, and being relatively amenable to transformation and genetic manipulation. Stress responses in *S. cerevisiae* are one particularly well-studied area, and many investigations into the dynamics of histone

modifications in these processes have been carried out. This report shall focus on the osmotic stress response.

Exposure to high osmolarity in *S. cerevisiae* induces water loss, cell shrinkage and changes in the concentration of key ions such as Na⁺ (Saito and Posas, 2012). The organism responds to these challenges by arresting the cell cycle, adjusting transcription patterns and increasing synthesis of glycerol (Saito and Posas, 2012). The major regulator of these responses is the MAPK *HOG1*, which accumulates in the nucleus following osmotic stress and is able to integrate transcriptional responses at various stress-responsive loci (Alepuz et al., 2003, Saito and Posas, 2012). The importance of *HOG1* in the response is shown by the observation that 80% of loci responsive to osmotic stress are dependent upon *HOG1* for this response (Saito and Posas, 2012).

HOG1 has been identified to interact with chromatin via association with transcription factors, and only shows recruitment to gene loci which show changes in transcription upon osmotic stress (Saito and Posas, 2012). *HOG1* serves to recruit transcriptional machinery and other transcription factors to these loci, and this seems to be the major mechanism by which *HOG1* influences transcription (Alepuz et al., 2003). The usual MAPK mechanism of activating transcription, namely phosphorylation of downstream transcription factors, seems dispensable in this pathway (Alepuz et al., 2003). One of the major factors that *HOG1* recruits during osmotic stress is a histone deacetylase known as *RPD3*, which is recruited to stress-responsive gene loci in a *HOG1* dependent

fashion during osmostress (De Nadal et al., 2004) and forms the main focus of research in this report.

1.3 The *RPD3* Histone Deacetylase

1.3.1 Canonical and Recent Roles of *Rpd3*

RPD3 (Reduced Potassium Dependency three) is a well-studied histone deacetylase originally identified in a screen for *S. cerevisiae* strains with increased potassium transport (Vidal et al., 1990). It is known to catalyse removal of acetyl groups from lysine residues on all four core histones (De Nadal et al., 2004). *RPD3* has been well studied since its discovery, and is implicated in a number of cellular roles, particularly stress responses (Schroder et al., 2004, Mas et al., 2009, McDaniel and Strahl, 2013) and cell cycle progression (Guarente and Kenyan, 2000, Schroder et al., 2004, Gajan et al., 2016).

RPD3 is canonically known as a transcriptional repressor, in accordance with the canonical view of histone deacetylation. The roles of *RPD3* in transcriptional repression are well established and continue to be cited in the literature (Kadosh and Struhl, 1997, Kadosh and Struhl, 1998, Schroder et al., 2004, Keough et al., 2005, Stuparevic et al., 2015). However, as discussed previously for histone acetylation and histone modifications more widely, it may be an over-simplification to assume this is the sole role of *RPD3*. Indeed, numerous observations in the literature have challenged this canonical role. The first of these reports were made in the 1990s, finding that deletion of *RPD3* leads to defects in transcriptional *activation* as well as repression (Vidal and Gaber, 1991, Rundlett et al., 1996, Pazin and Kadonaga, 1997). These were backed up

by further reports in the 21st century investigating the molecular details of transcriptional regulation at *RPD3*-regulated loci (De Nadal et al, 2004, Oakes et al, 2006), as well as citations that *RPD3* homologues in other systems are also involved in transcriptional activation (Zupkovitz et al, 2006). Perhaps most notable is the observation by (De Nadal et al., 2004), that point mutations affecting Rpd3's deacetylase activity had the same effect as deletion of the gene. This suggests that deacetylation is in some way required for gene activation, providing a direct challenge to the canonical view of deacetylation (De Nadal et al., 2004).

It must be noted that some of these reports, particularly the earlier ones (Vidal and Gaber, 1991, Rundlett et al., 1996, Pazin and Kadonaga, 1997) could potentially be explained by an indirect mechanism in which *RPD3* acts to repress the expression of a third factor, a transcriptional repressor. This repressor would be hypothesised to repress expression of the *RPD3*-activated genes, thus explaining how its inhibition by *RPD3* would result in the expression of these genes. However, later reports analysed the recruitment of Rpd3, and found that it was localised in a *HOG1*-dependent manner to the promoters of genes which showed *RPD3*-dependent gene activation during stress responses (De Nadal et al., 2004, Zapater et al., 2007). Furthermore, it has also been identified that *RPD3* is required for recruitment of transcriptional activators at the promoters of genes expressed under anaerobic conditions during the *S. cerevisiae* hypoxia stress response (Sertil et al., 2007). These observations are not what would be expected if *RPD3* was functioning to activate genes indirectly via a repressive action at other gene loci. Whilst they do not eliminate the possibility of indirect action via

inhibition of an external repressor, they are more consistent with *RPD3* playing some positive roles in transcriptional activation at genomic locations to which it is recruited.

As aforementioned, it is known that stress responses represent one of the most crucial areas of *RPD3* activity in the cell. It is also in this area that *RPD3* has been identified as a requirement for transcriptional activation, rather than repression. This makes stress responses ideal area to study for new insights into how histone modifications govern transcription in general. *RPD3* has been identified as being required for full transcriptional responses to osmotic stress (De Nadal et al., 2004, Mas et al., 2009), oxidative stress (Alejandro-Osario et al., 2009), heat shock (Loewith et al., 2001, Ruiz-Roig et al., 2010) and hypoxia (Sertil et al., 2007). The latter of these (Sertil et al., 2007) is perhaps the most striking, as this report found that *RPD3* was required for recruitment of transcriptional activators. This is most suggestive of *RPD3* playing a positive role in gene activation at *RPD3*-binding locations, rather than indirect effects via external loci, as discussed previously. More recently, *RPD3* has also been implicated in resistance to azole stress (Li et al., 2012) and *rpd3Δ* mutants have displayed increased sensitivity to disruption of protein synthesis (Kugler et al, 2015). However, despite the intense research in this area, there are still unanswered questions, particularly relating to the mechanism of action of *RPD3*, and how it promotes transcriptional responses in these pathways.

One particular question regards the context of *RPD3* action to induce transcription. *RPD3* is well known to carry out histone deacetylation, and this deacetylase activity has been identified as required for full *RPD3*-mediated induction of transcription (De Nadal et al., 2004). However, there is conflict in the literature about the precise level of

deacetylation observed during the process. In (De Nadal et al., 2004), the authors identify an overall decrease in acetylation levels in up-regulated genes during the osmotic stress response, and conclude that *RPD3*-mediated deacetylation induces gene expression. The mechanistic basis of how this happens is not addressed in this publication. However, a more recent report has found opposing results, observing a rise in acetylation levels during *RPD3*-mediated induction of transcription (Magraner-Pardo et al., 2014) – a finding in agreement with previous unpublished work in the Schroder laboratory. The difference in these findings may be down to a difference in how chromatin immunoprecipitation-quantitative PCR data is normalised. The authors of (De Nadal et al., 2004) cross-linked chromatin to DNA and precipitated this complex with antibodies targeting histone 3 acetylated at lysine 9 (H3K9Ac), before measuring the enrichment of certain genes before and after osmotic stress via qPCR. The data was calibrated by also carrying out qPCRs targeting telomeres, to account for differences in the total amount of DNA present in different samples (De Nadal et al., 2004). However, calibration against other genomic locations whilst measuring changes in histone acetylation means that potential changes in histone occupancy are not considered, which can introduce error into the results. Unpublished data in the Schroder laboratory and the authors of (Magraner-Pardo et al., 2014) both take into account nucleosome occupancy by carrying out a parallel immunoprecipitation utilising antibodies targeting H3 regardless of acetylation activity. This technique is admittedly complex, but observations since De Nadal et al., 2004 have suggested that changes in histone occupancy are important, and thus calibration of ChIP-qPCR data using external genomic sites is inappropriate. In 2005 it was found that nucleosome occupancy was inversely correlated with transcriptional activity at a gene, with

nucleosomes removed during transcriptional activation, particularly near the promoters of actively transcribed genes (Poklohoc et al., 2005). Notably, this paper actually observed a distinct drop in nucleosome occupancy at promoters of oxidative stress-responsive genes after induction of oxidative stress (Poklohoc et al., 2005). This suggests that normalisation of ChIP data via genomic DNA is not appropriate when analysing acetylation of histones during stress responses, a conclusion particularly reinforced by another observation during this paper. The authors find that acetylation at H3K9 and H3K14 increases near the transcriptional start sites of genes alongside transcriptional activation, but reference a previous paper (Kurdistani et al., 2004) which found no such correlation. The authors of (Poklohoc et al., 2005) find that their data agreed with that in (Kurdistani et al., 2004) when they stopped accounting for nucleosome occupancy and normalised their ChIP data using genomic DNA rather than core histones. This result provides strong evidence that differences in nucleosome occupancy may have a marked effect on levels of acetylated histone observed, and therefore must be accounted for when analysing histone acetylation, despite the additional complexity introduced by carrying a second immunoprecipitation.

Thus, it can be hypothesised histone loss is occurring during transcriptional induction to osmotic stress alongside histone acetylation, which may explain the different conclusions in (De Nadal et al., 2004), (Magraner-Pardo et al., 2014) and previous unpublished work in the Schroeder laboratory. Further observations since (De Nadal et al., 2004) offer further evidence for this hypothesis, with a report in 2009 finding distinct nucleosome depletion alongside hyperacetylation of histones at stress-

responsive genes during osmotic stress responses in mammalian cells (Tong et al., 2009).

This hypothesis would also mean that an overall increase in acetylation is occurring despite the deacetylase activity of *RPD3*. This would indicate other factors at work during the stress response and could potentially indicate that *RPD3* is having an indirect effect on transcription via recruitment of other chromatin modifying proteins, rather than a direct effect via decreasing acetylation levels. This view (namely that *RPD3* has an indirect effect via recruitment of other chromatin modifying proteins) has been proposed in the literature (Saito and Posas, 2012). In any case, however, further studies on the changes in acetylation observed during stress responses would be beneficial in resolving this conflict. Another unanswered question is whether the mechanism of action is conserved among different stress responses, or whether *RPD3* induces transcription in a stress-specific fashion. There is evidence that *RPD3* functions alongside the same interactive partners (discussed in more detail below) in the responses to heat shock and oxidative stress (Loewith et al., 2001, Alejandro-Osario et al., 2009, Ruiz-Roig et al., 2010). However, this analysis has not been carried out in oxidative stress responses, so further studies in this area would be useful for increasing confidence that *RPD3* action is conserved among stress responses. Both of these areas (the changes in acetylation during *RPD3*-mediated transcriptional induction and the interactive partners functioning in the process) will be addressed in this report.

1.3.2 Regulation of *RPD3* Activity

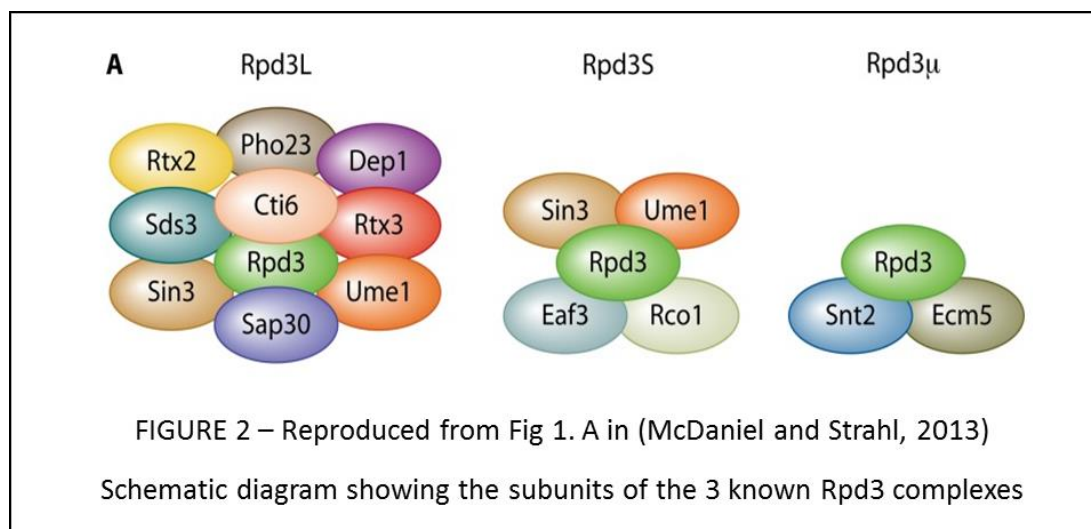
Along with mechanism of action, the regulation of *RPD3* activity remains a key area of active research. A generally accepted view is that recruitment of Rpd3 to specific

genomic loci is one major part of this regulation, with *RPD3* not found to have global effects on transcription across the genome. Targeting of Rpd3 to specific promoters has been cited as a method of affecting expression levels of the genes in question (Deckert and Struhl, 2002). Equally, numerous findings in the literature have found roles of different factors in performing this recruitment, and found this to be key in modulation of expression at certain loci (Kadosh and Struhl, 1997, De Nadal et al., 2004, Mas et al., 2009).

Another major factor in *RPD3* regulation is its association with different interactive partners, which also serves as a key modulator of the precise location to which *RPD3* is localised. Perhaps the most important of these is Sin3, sometimes referred to as a “co-repressor” alongside *RPD3* (Kadosh and Struhl, 1997). Sin3 has long been recognised as a crucial factor for *RPD3* activity, and is often discussed concurrently with *RPD3* in the literature (Kadosh and Struhl, 1997, Schroder et al., 2004, Gajan et al., 2016). As further investigation into *RPD3* was carried out, two major protein complexes were identified, both having *RPD3* and Sin3 as key members. These complexes were first characterised in 2005, and were termed the Large complex (Rpd3L) and the small complex (Rpd3S) after their respective molecular weights of 1.2 MDa and 0.6 MDa (Carrozza et al., 2005). In 2013, a third, novel *RPD3* complex was discovered, and termed the micron complex (Rpd3 μ) (McDaniel and Strahl, 2013). These 3 known

complexes are schematically illustrated in Figure 2 (reproduced from McDaniel and Strahl, 2013).

The two more established *RPD3* complexes (Rpd3L and Rpd3S) have distinct profiles of recruitment and action. Rpd3L has been found to be recruited to promoters by sequence-specific transcription factors, whilst Rpd3S is mainly recruited to open reading frames, via the Rco1 and Eaf3 subunits (Alejandro-Osario et al., 2009,



Yehesekely-Hayon et al., 2013). Rpd3 μ , having only been discovered in 2013, is unsurprisingly less well characterised, with a limited number of studies carried out to date on this complex (Baker et al., 2013, McDaniel and Strahl, 2013). In analyses of Rpd3L and Rpd3S, literature reports have consistently found that Rpd3L is required for the transcriptional response to stresses, whilst Rpd3S is dispensable. The first such findings emerged in 2001, finding that the Rpd3L subunit encoded by *PHO23* was required for full transcriptional responses to heat shock (Loewith et al., 2001). Further studies later found consistent results that *PHO23* was required for responses to both heat shock and oxidative stress (Alejandro-Osario et al., 2009, Ruiz-Roig et al., 2010). Meanwhile RCO1, a subunit of the Rpd3S complex, was found to be dispensable, and

strains carrying *rco1Δ* deletions did not show defects in transcriptional responses to these stresses (Alejandro-Osario et al., 2009, Ruiz-Roig et al., 2010). It has also been observed in the literature that strains carrying deletions in Rpd3L subunits have shown increased sensitivity to osmostress (Saito and Posas, 2012), which is consistent with *RPD3* functioning via the large complex in this stress response. This latter report also proposed the view that *HOG1* is most likely to recruit Rpd3 via interaction with the large complex (Saito and Posas, 2012).

The discovery of the Rpd3 μ complex, however, has complicated this matter somewhat. Firstly, the Rpd3 μ complex subunit *SNT2* has been found to be required for full responses to oxidative stress (Baker et al., 2013). This raises the possibility that *RPD3* may function through several pathways simultaneously, adding an extra layer of complexity to its function. Secondly the other Rpd3 μ subunit, *ECM5*, was not found to be required for transcriptional activation in this report, posing new questions as to how members of the same protein complex mediate differing transcriptional processes. However, it is possible that *SNT2* may be acting independently of Rpd3, and that the Rpd3 μ complex simply does not function in this process. Analysis in other stress responses to detect if these results are consistent would be useful in this regard. Alongside these new questions posed by Rpd3 μ , it must also be noted that a complex-specific analysis of transcription has not been carried out in the osmotic stress response. This type of analysis would be useful to identify how fully conserved *RPD3* action is across its different roles. Thus, this report shall address the complex-specificity of Rpd3's known role in osmotic stress responses. Equally, it would be useful to investigate how histone acetylation patterns in this stress response respond to loss

of the various *RPD3* complexes. If a correlation is observed between transcriptional defect and an acetylation signature, it will help elucidate the key functions behind Rpd3-mediated transcriptional induction.

1.4 Experimental Hypotheses and Objectives

As discussed, *RPD3* is known to function in the osmotic stress response and a complex-specific analysis of this function, missing in the literature, is a logical step for further studies of Rpd3. Previous work in the Schroder group (unpublished) has suggested that Rpd3L was required for full transcriptional induction of these genes, whilst Rpd3S was dispensable. However, only one subunit of Rpd3L has been tested, limiting the confidence in these results, particularly in light of recent findings that different Rpd3 μ subunits have different effects in stress responses (Baker et al., 2013). As aforementioned, the Schroder laboratory has also found an increase in acetylation at genes upregulated in response to osmotic stress. This is in agreement with (Magraner et al., 2014), but conflicts with (De Nadal et al., 2004), possibly due to a difference in how the data is normalised.

This thesis will investigate the role of *RPD3* in the osmotic stress response, with a view to corroborating and extending this previous unpublished work. The research will focus on a set of well characterised proteins: Genes de Respuesta a Estres 2 (*GRE2*), Heat Shock Protein 12 (*HSP12*), Sugar Transporter-Like protein 1 (*STL1*); CaTalase T (*CTT1*) and Aldehyde Dehydrogenase (*ALD3*). These proteins are known to be transcriptionally upregulated in response to osmotic stress (Soufi et al., 2009, Raffaello et al., 2012), and thus make ideal targets for investigating how *RPD3* modulates transcription in this stress response.

The first requirement for this complex specific analysis was to generate *S. cerevisiae* strains carrying deletions for Rpd3 μ subunits Snt2 and Ecm5. These gene deletions were carried out using the well-established method of PCR-mediated gene deletion, first described in 1993 (Baudin et al., 1993). The G148 resistance cassette kanMX2 was used as a selective marker.

With a full complement of deletion mutants for the three *RPD3* subunits available, the first experimental objective was to provide robust evidence showing which of the three *RPD3* complexes was required for transcriptional responses to osmotic stress. Based on previous work, both published and unpublished, I hypothesise that strains carrying deletions in Rpd3L subunits will be defective in the osmotic stress response, whilst those carrying deletions in Rpd3S-specific subunits will be unimpaired.

Hereafter, strains carrying deletions in Rpd3L subunits shall be collectively referred to in the text as *rpd3L Δ* strains, whilst those carrying deletions in Rpd3S subunits shall be collectively referred to as *rpd3S Δ* strains. Strains carrying deletions in Rpd3 μ subunits shall be collectively referred to as *rpd3 μ Δ* strains. Northern blotting was used to analyse the expression of genes upregulated during the osmotic stress response (*GRE2* and *CTT1*), in both WT strains and in strains carrying deletions in specific subunits spanning the three complexes. *rpd3L Δ* show evidence of a defect in the osmostress-induced transcriptional upregulation of these genes, which is not as apparent in *rpd3S Δ* strains. However, technical challenges encountered with the procedures mean this evidence is not conclusive, which shall be discussed in detail with regards to these results.

The second experimental objective is to investigate the molecular basis of transcriptional upregulation by characterising the changes in histone acetylation occurring during osmotic stress. Again, based on previous data in the Schroder laboratory and (Magraner-Pardo et al., 2014), we expect to find an overall increase in acetylation at genes which are upregulated during osmotic stress. I also hypothesise that this acetylation may be absent or impaired where transcriptional upregulation is defective (proposed to be in strains carrying deletions in Rpd3L subunits). Such a correlation between acetylation and transcriptional upregulation would be consistent with the notion of an overall increase in acetylation having an active effect on gene expression. Another interesting possibility is that different acetylation sites may show different patterns of acetylation. The authors of (Magraner-Pardo et al., 2014) found that acetylation at histone 3 lysine 9 (H3K9Ac) correlated well with Pol II occupancy in gene bodies and was thus predictive of transcription, whereas acetylation at histone 4 lysine 8 (H4K8) did not show such strong correlation (Magraner-Pardo et al., 2014). Such site-specific acetylation correlating with transcriptional activation is again consistent with the notion of a mechanistic link in this process, rather than simply a by-product of some globalised acetylation effects across the genome. Chromatin Immunoprecipitation-quantitative PCR (ChIP-qPCR) is used to analyse the acetylation levels at these 2 residues (H3K9 and H4K8) before and after osmotic stress, with the data normalised against total H3 to account for histone occupancy. Total H3 data is then normalised against data from non-immunoprecipitated DNA, to discern the change in total Histone occupancy. Evidence is obtained of an increase in histone acetylation at osmostress-induced genes in WT strains after osmotic stress, alongside a

decrease in total H3 occupancy. The data suggest that Rpd3L subunits are required for these effects to occur, but that Rpd3S subunits are not.

Chapter 2 – Materials and Methods

2.1 Reagents and Chemicals

Most chemical reagents used in this study were purchased from Fisher Scientific, Loughborough, UK. All YPD medium was purchased from Formedium, Hunstanton, UK. Table 1 details suppliers for chemical reagents used in this study. The composition of reagents prepared in the laboratory are detailed the first time they are referred to in the text.

The primers used in this study are listed in Table 2.

Table 1 – Details of suppliers for chemical reagents used in this study	
Reagent	Supplier
2.5mM MgCl ₂	Promega UK, Southampton
5X Colorless GoTaq Flexi buffer	Promega UK, Southampton
Agar	Formedium, Hunstanton
Agarose	Bioline, London
Bacto Yeast Extract	Fisher Scientific, Loughborough
Bacto-Peptone	Difco Laboratories, Detroit, USA
Diethyl pyrocarbonate	Fisher Scientific, Loughborough
DMSO	Sigma-Aldrich, Irvine
Ethanol	Fisher Scientific, Loughborough
Formamide	Fisher Scientific, Loughborough
G418	Formedium, Hunstanton
Glycerol	Fisher Scientific, Loughborough
Glycine	Fisher Scientific, Loughborough
Glyoxal	Sigma-Aldrich, Irvine
GoTaq Flexi Polymerase	Promega UK, Southampton
NaCl	Fisher Scientific, Loughborough
NaOAc	Fisher Scientific, Loughborough
Phenol:Chloroform:Isoamylalcohol	Fisher Scientific, Loughborough
Potassium Acetate	Acros Organics, Thermo Fisher Scientific, Geel, Belgium
Salmon sperm DNA	Fisher Scientific, Loughborough
SDS	Fisher Scientific, Loughborough
Sorbitol	Melford, Suffolk
Sybr Green	Fisher Scientific, Loughborough
YPD Broth	Formedium, Hunstanton
YPD Agar	Formedium, Hunstanton

Table 2 – List of primers used in this study	
Primer used for	Sequence
<i>ECM5</i> deletion, 5' primer	TCTAGATTATCGTGTATGTTCTTGTTTCGTACGT CCATCTCCATAGTTATAAAGCTTCGTACGCTGC AGGT
<i>ECM5</i> deletion, 3' primer	GTATGCGCAATAAAAGAAGAGAGAATATGTCAT GCAGACTTCGCAGGTACATAGGCCACTAGTGGATCTG
<i>ecm5</i> deletion screening #1	TCTAAGACTTCCATCCGTGC
<i>ecm5</i> deletion screening #2	ATTGTTTCAGGTGCAAACGG
<i>SNT2</i> deletion 5' primer	TTGGCCTATCGGGACATATTGAGATCATCTGCC TTTCAGCTGGTCACGCTAAGCTTCGTACGCTGC AGGT
<i>SNT2</i> deletion 3' primer	AAGCCGCGCAAGATTGGACCATACTTTCTATCT AAGGTAACTATCACTTAATAGGCCACTAGTGGATCTG
<i>snt2</i> deletion screening #1	TGGTGTCAATTGAAACAGTAGACG
<i>snt2</i> deletion screening #2	GCAATTTGAGATCAGGTGCC
Ctt1 q-PCR_F Primer	CGTATCCCCTACTGCTACACG
Ctt1 q-PCR_R Primer	ACCGAACACGTTCAATTGTG
Ald3 q-PCR_F Primer	AAAATGGCAAATCTGGATG
Ald3 q-PCR_R Primer	TTTTCAATTGTGGGATTTTCG
Hsp12 q-PCR_F Primer	GAGGGGAAAAGGAAAAGGAAAAG
Hsp12 q-PCR_R Primer	GAGGAAGTAGAACGCAATTC
Stl1 q-PCR_F Primer	TTGCAGTTCAGGAGTAGTCACA
Stl1 q-PCR_R Primer	AAATTTGCCTTTGAAATTCGAT
<i>CTT1</i> Northern Blot Probe_F	TAATTGGCACTTGCAATGGA
<i>CTT1</i> Northern Blot Probe_R	GACTTCGAACAGCCAAGAGC
<i>GRE2</i> Northern Blot Probe_F	CAGCTACCTGGGAGAGTTGC
<i>GRE2</i> Northern Blot Probe_R	TCCGGTATCTTGTCCTCTGG

2.2 Culturing of Yeast Strains

2.2.1 Strains Utilised in this Study

All strains in this study are haploid *S. cerevisiae* derived from the SK-1 strain (Kane and Roth, 1974). Two wild type strains are used, which were previously described in (Schröder et al., 2004). All other strains used are derived from one of these strains, and were created using the same PCR-mediated described in Chapter 2.3. Strains used are listed below.

Strain Name	Shorthand	Genotype	Reference
MSY 136-40	WT	SK-1 MAT α <i>arg6</i> <i>rme15Δ::LEU2</i> <i>ura3Δ</i> <i>leu2Δ::hisG</i> <i>trp1Δ::hisG</i> <i>lys2Δ</i> <i>hoΔ::LYS2</i>	(Schröder et al., 2004)
MSY 136-36	WT	SK-1 MAT α <i>arg6</i> <i>rme15Δ::LEU2</i> <i>ura3Δ</i> <i>leu2Δ::hisG</i> <i>trp1Δ::hisG</i> <i>lys2Δ</i> <i>hoΔ::LYS2</i>	(Schröder et al., 2004)
JN1	<i>rpd3Δ</i>	MSY 136-40 <i>rpd3Δ::kanMX21</i>	Schröder laboratory strain inventory (Unpublished)
JN2	<i>sin3Δ</i>	MSY 136-40 <i>sin3Δ::kanMX21</i>	Schröder laboratory strain inventory (Unpublished)
JN3	<i>sap30Δ</i>	MSY 136-40 <i>sap30Δ::kanMX2</i>	Schröder laboratory strain inventory (Unpublished)
JN4	<i>dep1Δ</i>	MSY 136-40 <i>dep1Δ::kanMX2</i>	Schröder laboratory strain inventory (Unpublished)
JN5	<i>cti6Δ</i>	MSY 136-40 <i>dep1Δ::kanMX2</i>	Schröder laboratory strain inventory (Unpublished)
JN6	<i>pho23Δ</i>	MSY 136-40 <i>pho23Δ::kanMX2</i>	Schröder laboratory strain inventory (Unpublished)
JN7	<i>rxt2Δ</i>	MSY 136-40 <i>rxt2Δ::kanMX2</i>	Schröder laboratory strain inventory (Unpublished)

JN8	<i>rxt3Δ</i>	MSY 136-40 <i>rxt3Δ::kanMX2</i>	Schröder laboratory strain inventory (Unpublished)
JN9	<i>rpd3Δ</i>	MSY 134-36 <i>rpd3Δ::kanMX2</i>	Schröder laboratory strain inventory (Unpublished)
JN10	<i>sin3Δ</i>	MSY 134-36 <i>sin3Δ::kanMX2</i>	Schröder laboratory strain inventory (Unpublished)
JN11	<i>rco1Δ</i>	MSY 134-36 <i>rco1Δ::kanMX2</i>	Schröder laboratory strain inventory (Unpublished)
JN12	<i>eaf3Δ</i>	MSY 134-36 <i>eaf3Δ::kanMX2</i>	Schröder laboratory strain inventory (Unpublished)
JN13	<i>ecm5Δ</i>	MSY 134-36 <i>ecm5Δ::kanMX2</i>	Generated in this study
JN14	<i>snt2Δ</i>	MSY 134-36 <i>snt2Δ::kanMX2</i>	Generated in this study

2.2.2 Storage and Culturing of Yeast Strains

YPD medium purchased from Formedium, Hunstanton, UK was used for all culturing unless stated otherwise. YPD broth was prepared according to manufacturer's instructions, then autoclaved at 121°C for 20 min. If NaCl or sorbitol was to be present in the media, this was added prior to autoclaving.

All strains were revived from frozen stocks prepared as follows: 1 ml of cell culture grown to saturation in YPD broth, and transferred to sterile 2 ml cryotubes. 1 ml of 30% (w/v) glycerol added. Cells were resuspended by vortexing, appropriately labelled and flash frozen in liquid N₂, then stored at -80°C

For use in experiments, strains were revived onto appropriately labelled YPD agar

plates and grown for 2-3 days at 30°C until colonies of a suitable size had formed.

Plates were kept at 4°C for 1-2 months before being discarded, and new cultures revived from frozen stocks.

For all experiments, cell cultures were grown as follows. Cultures taken from YPD agar plates using sterile toothpicks and transferred into 12 ml culture tubes containing 2-4 ml of YPD broth. The cells were grown to saturation (1-3 days for *S. cerevisiae* in YPD broth) in a shaking incubator at 30°C. The optical density OD₆₀₀ of this culture was measured, and diluted to a low OD in appropriate volume of YPD. These cultures were then grown to mid-log phase at 30°C, in baffled culture flasks:

- For northern blotting experiments, cultures of 40 – 70 ml were grown to OD 0.3 < OD₆₀₀ < 0.8
- For Chromatin immunoprecipitation and cell transformations, cultures of 200-300ml grown OD of 0.8 < OD₆₀₀ < 1.2
- For cell transformations for PCR-mediated gene deletions, cultures of 30ml were grown to 0.8 < OD₆₀₀ < 1.2

For Northern Blotting and Chromatin Immunoprecipitation, cultures were then split into control and treatment groups in 50ml falcon tubes as follows

- For northern blotting experiments, 15-20ml culture aliquots taken for control group and each treatment group
- For Chromatin immunoprecipitation experiments, culture aliquots of 80-100ml taken for control group and each treatment group

Cells are then pelleted by centrifugation for 2 min at 3750g. For treatment groups, supernatant discarded and cells resuspended in same volume of YPD containing NaCl or sorbitol to a given concentration. For control groups, cells were simply resuspended without exchange of media. Cells then transferred to clean non-baffled culture flasks and incubated for given length of time at 30°C with shaking.

2.3 PCR-Mediated Gene Deletion

Figure 3 schematically illustrates the protocol used for carrying out PCR-mediated gene deletion of *ECM5* and *SNT2* genes. Two cultures of MSY134-36 were each transformed separately with deletion constructs targeting the *SNT2* and *ECM5* genetic loci, the two subunits of the Rpd3 μ complex (McDaniel and Strahl, 2013). Genomic sequences for relevant genes (*Snt2* and *Ecm5*) were obtained from the Saccharomyces Genome Database (<http://www.yeastgenome.org/>) and analysed using pDRAW32 software. Primers were designed using PRIMER3 software (Koressaar and Remm, 2007) to incorporate 50bp of sequence homologous to the ORF of the gene in question, and 20bp of sequence homologous to a pFA6a-kanMX2 plasmid containing a G418 resistance marker (kanMX), as illustrated in Figure 3. For each gene, primers were also designed to test the presence of the deletion construct, and the absence of the WT gene, using pDRAW32 and PRIMER3 software. These primers are schematically illustrated in Figure 4. Primers sequences are detailed in Table 2.

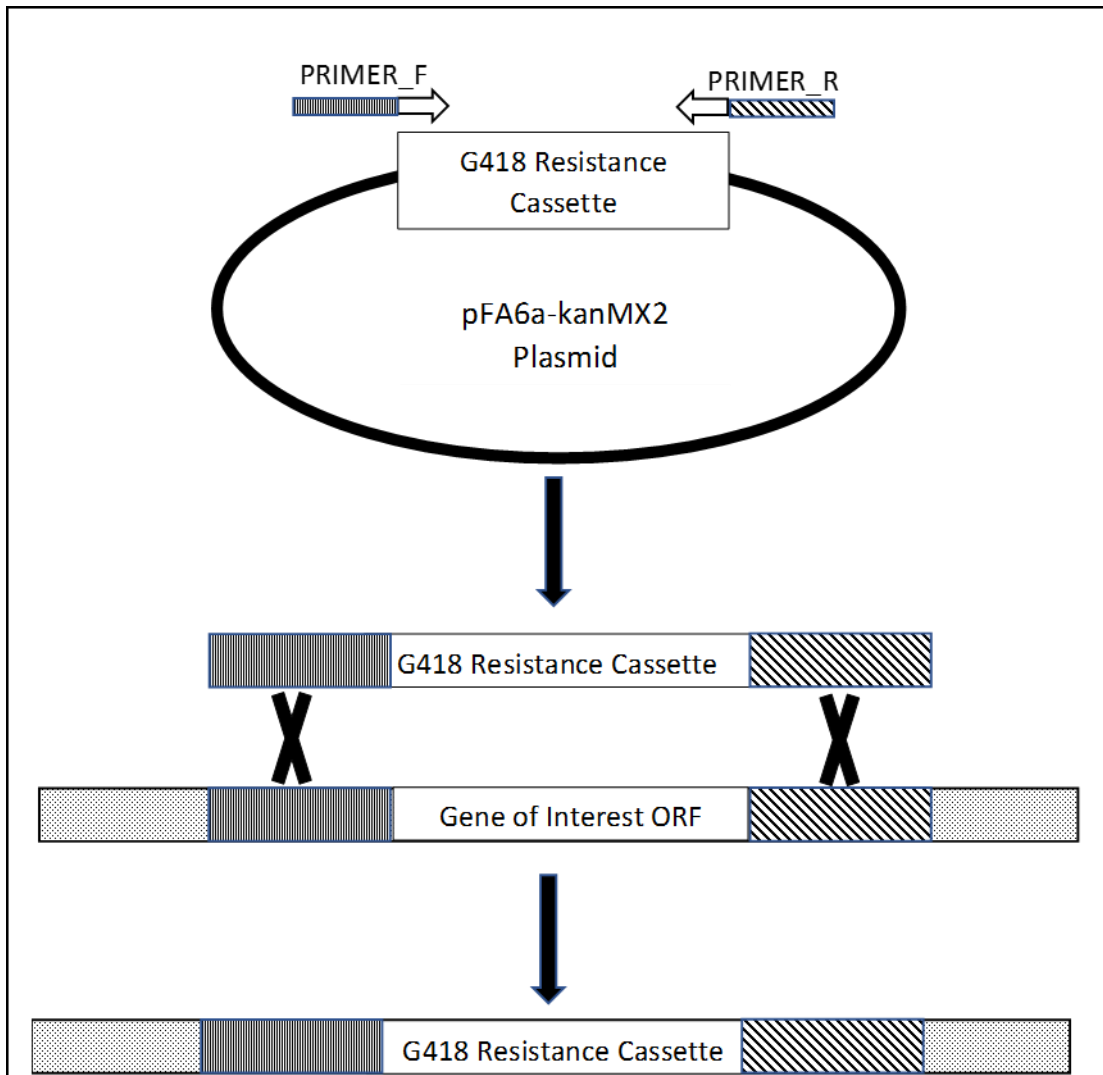


Figure 3 – Schematic illustration of PCR-mediated gene deletion methodology

Figure 3 illustrates the mechanism by which gene deletions were induced in in *ECM5* and *SNT2* loci. A PCR amplification using primers as shown was carried out to produce a deletion construct. PRIMER_F and PRIMER_R are representative of “*ECM5* deletion, 5’ primer” and “*ECM5* deletion, 3’ primer” respectively, for inducing deletions at the *ECM5* loci. For inducing deletions at the *SNT2* loci, PRIMER_F and PRIMER_R represent “*SNT2* deletion, 5’ primer” and “*SNT2* deletion, 3’ primer”, respectively. The sequences for these primers are detailed in Table 2. Once a deletion construct was amplified by PCR, it was then transformed into *S. cerevisiae* strains, and would replace the WT ORF via homologous recombination, as shown. This gave a strain lacking the WT ORF for the gene in question, and selectable via a G418 resistance marker.

The deletion construct was amplified by PCR using the pFA6a-kanMX2 plasmid as template DNA. The PCR mix consisted of the following reagents, made up to 100µl with sterile H₂O

- 25ng pFA6-a-kanMX2 plasmid template DNA
- 20µL 5X Colourless flexi Buffer
- 8µL 2.5mM MgCl₂
- 10µL 2mM dNTP
- 0.5µM of each Primer
- 1µL 5units/µL GoTaq Flexi Buffer

A PCR was then run (2 minutes at 95°C, followed by 30 cycles of [95°C for 30 seconds, 55°C for 30 seconds, 72°C for 90s]). The PCR product was ran on a 1% (w/v) Agarose gel to confirm presence of a product of correct size, and the DNA was then precipitated by adding 1/10 Vol 3M NaOAc (Ph5.2) and 3 Vol ethanol. This was incubated overnight at -80°C and collected by centrifugation for 30min at 12,000g, 4°C. The supernatant was removed. The DNA was washed once with ice-cold ethanol, then re-pelleted by centrifuging for 15min at 12,000g, 4°C. The supernatant was removed and the pellet dried at room temperature and then dissolved in 1xTE buffer (10 mM Tris·HCl (pH 8.0), 1 mM EDTA). This DNA formed the deletion construct to be used to induce genetic disruptions in Rpd3µ subunits.

S. cerevisiae strains were then cultured as described in Chapter 2.2, and transformed using 30µg of the deletion construct DNA as via LiOAc transformation (Chen et al., 1992). The cell pellet, collected as described in Section Chapter 2.2, was resuspended in 5-10ml one step buffer (0.2 M LiOAc, 40% (w/v) PEG4000), then centrifuged again at

3750g for 2 minutes, and the supernatant discarded. The cell pellet was resuspended in 88µL one-step buffer and then added to tubes containing transforming 30µg transforming DNA and 100 µg sheared salmon sperm DNA. This mixture was then incubated at 42°C for 30 min. The cells were then placed on ice, collected by centrifugation, and resuspended in 200µL H₂O.

After the transformation was complete, the cells were plated on YPD agar, left to grow for 1 day and then replica plated onto YPD Agar plates containing 400mg/ml G418. These plates were left to grow for 2 days then checked for successful colony growth, with the hypothesis that any G418 resistant colonies should contain the deletion construct. G418-resistant colonies were obtained from both transformations. All colonies were re-grown on YPac agar plates (1% (w/v) bacto-yeast extract, 2% (w/v) bacto-peptone, 2% (w/v) KOAc, 2% (w/v) agar). This step was carried out to identify and eliminate from the study *petite* mutant strains. These plates were left to grow for 2-3 days and then checked for growth, with any colonies not showing growth on this medium eliminated from the study. Colonies showing growth on both G418-YPD and YPac plates were obtained from each transformation. Several from each transformation were selected for genotyping to verify correct insertion of the deletion construct.

Genotyping PCR was then carried out to verify presence of the deletion construct and absence of WT loci for the gene in question. Two PCRs were carried out for each colony genotyped. The first of these PCRs made use of primers targeting sequences inside the deletion construct and outside of the locus being targeted, and thus

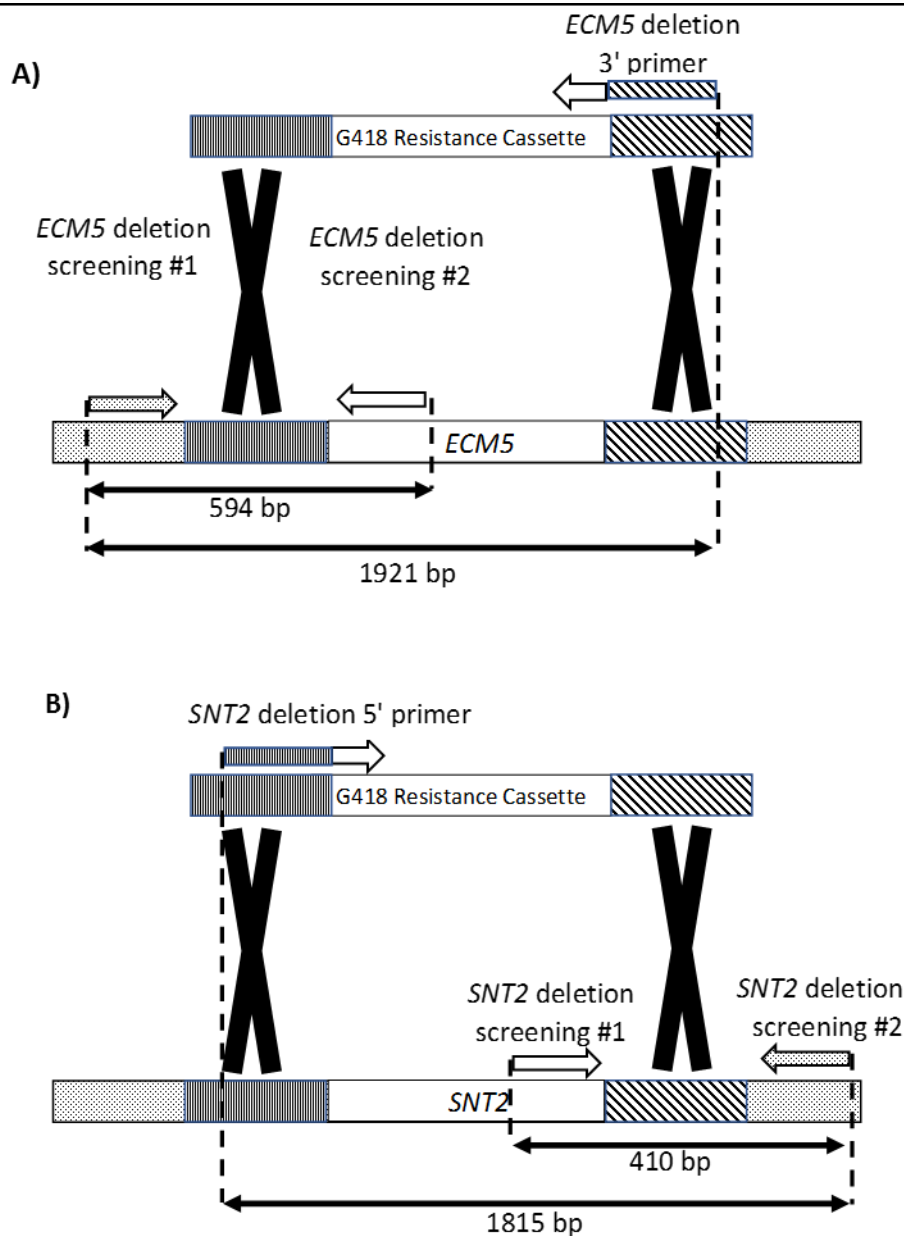


Figure 4 – Schematic illustration of PCR genotyping of mutants transformed with deletion constructs for *ECM5* and *SNT2*.

Figure 4 illustrates how PCR genotyping was used to verify successful PCR-mediated gene deletion of *ECM5* (A) and *SNT2* (B). (A) DNA from strains transformed with deletion constructs targeting the *ECM5* locus was used as template for 2 PCR reactions. The first used primers “*ECM5* deletion screening #1” and “*ECM5* deletion 3’ primer”, and produced a product of 1921bp if the deletion construct had successfully integrated into the genomic DNA at the *ECM5* locus. The 2nd PCR used primers “*ECM5* deletion screening #1” and “*ECM5* deletion screening #2”, and produced a product of 594bp if the WT locus for *ECM5* was present. (B) DNA from strains transformed with deletion constructs targeting the *SNT2* locus was used as template for 2 PCR reactions. The first used primers “*SNT2* deletion 5’ primer” and “*ECM5* deletion screening #2”, and produced a product of 1815bp if the deletion construct had successfully integrated into the genomic DNA at the *SNT2* locus. The 2nd PCR used primers “*SNT2* deletion screening #1” and “*SNT2* deletion screening #2”, and produced a product of 410 bp if the WT *ECM5* locus was present.

produced a product if the deletion construct had successfully integrated at the correct genomic locus (illustrated in Figure 4). The second PCR reaction made use of primers both inside and outside of the genomic locus being targeted for deletion, and thus produced a product if the WT locus was still present (Figure 4). Combining the information from these 2 PCRs allowed verification of successful integration of the deletion construct and absence of the WT locus, giving confidence that a strain lacking the target gene had been produced. The primer combinations used to carry out these genetic tests are illustrated in Figure 4. The PCR protocol was 2 minutes at 95°C, followed by 30 cycles of (95°C for 30 seconds, 55°C for 30 seconds, 72°C for 90s).

From each transformation, several colonies were obtained that showed presence of the deletion construct and absence of the WT locus for the target gene in question after PCR genotyping. These verifies that these colonies have the deletion construct integrated at the genomic locus for the target gene, and therefore do not possess a functional copy of that gene. Thus, *snt2Δ* strains and *ecm5Δ* strains have been successfully constructed. From these successfully transformed colonies, frozen glycerol stocks were prepared as described in Chapter 2.2.2. These colonies were labelled appropriately and stored at -80°C, ready for use in further experimentation.

2.4 Northern Blotting

2.4.1 RNA Extraction and Blotting Procedure

The northern blotting procedure has been described previously (Schröder et al., 2000). Cells were grown and stressed as described in Chapter 2.2, then transferred to 50ml falcon tubes and collected by centrifugation for 2 min at 3750g, 4°C. The supernatant was discarded. Cell pellets were washed with 1 ml Ice-cold DEPC-treated H₂O, then resuspended in 300µL RNA buffer (0.5 M NaCl, 0.2 M Tris·HCl (pH 7.5), 10mM EDTA). 100µg of 0.5mm glass beads (purchased from Thistle Scientific, Bothwell, catalogue #11079105) and 1 volume Phenol:Chloroform:Isoamylalcohol saturated with RNA buffer were added. Cells were lysed in a Precellys 24 cell homogenizer, using two 30-second cycles of 6000rpm, with a break of 15s. The nucleic acid extraction with 1 volume Phenol:Chloroform:Isoamylalcohol was repeated once, then nucleotides were precipitated by addition of 3 volume ethanol, and incubation at -80°C for >30 minutes. The RNA pellet was collected by centrifugation at 12000g for 2 minutes and washed once with 500µL ice-cold 70% (v/v) ethanol in DEPC-treated H₂O. RNA was dissolved in 50-100µL formamide and stored at -80°C. After extraction, RNA was quantified using a Warburg-Christian assay, with COSTAR 96-well plates.

For blotting, a 1.4% (w/v) agarose gel was cast, using 10mM Na_xH_{3-x}PO₄ as a buffer. Gel tanks were cleaned first using 2% (w/v) SDS. 10µg of RNA for each sample was resuspended in 50µL (1M Glyoxal, 50% v/v dimethyl sulfoxide, 10mM Na_xH_{3-x}PO₄) and denatured by incubating at 50°C for 1 hour. 1/6 volume 6X RNA buffer was then added, and the samples loaded onto the gel. The gel was ran at 100-120V for 3-4 h,

then cut to the desired size (discarding unused lanes and the area beyond where the loading dye had reached) using a scalpel.

RNA was then transferred to positively charged Zeta Probe GT Nylon membrane (purchased from Biorad, Watford, catalogue#162-0197), cut to the same size of the gel. A stack of paper towels was constructed, onto which were placed 4 sheets of whatman 3mm chromatography paper (Sigma Aldrich, Irvine, catalogue #WHA3030917), each cut to the same size as the gel. Sealing tape was placed down the edge of these papers to prevent short circuiting. An additional sheet of whatman 3 MM paper was soaked in 20X SSC (3 M NaCl, 0.3M Na₃-citrate), then placed on top of the other 4 papers. Then, the nylon membrane was briefly wet in DEPC-treated H₂O, before being soaked in 20X SSC and placed on top of the stack of whatman 3MM papers. The membrane was coated in 20X SSC and the gel was placed on top. 3 more whatman 3MM papers, cut to the size of the gel, were soaked in 20X SSC and placed sequentially on top of this stack. A final, larger piece of whatman 3MM paper was coated in 20X SSC and placed over the gel such that the stack was covered and this paper dipped into 2 trays of 20X SSC placed either side of the stack. The stack and trays were covered with clingfilm, and a glass plate was placed on top to apply weight to the construct. This was left overnight to allow the RNA to transfer to the membrane. Once RNA transfer was complete, it was cross-linked to the membrane via 1400W/cm² UV irradiation using a UVP CX-2000 crosslinker.

2.4.2 Hybridisation of Membranes

Membranes were first incubated at 65°C in 20mM Tris-HCl for 15 minutes to remove any remaining glyoxal. Membranes were then pre-hybridised for >3 hours at 42°C in

20ml Hybridisation Solution (50% (v/v) formamide, 5 x SSC, 0.1% (w/v) Ficoll 400, 0.1% (w/v) polyvinylpyrrolidone, 0.1% (w/v) BSA (fraction V), 1% (w/v) SDS, 100 µg/ml salmon sperm DNA (average size 2000 bp)). Membranes were then hybridised overnight at 42°C in 5ml Hybridisation solution containing labelled probes. The probes and method used to generate labelled probes is detailed in 2.4.3.

Membranes were then washed three times for 5 minutes with 2xSSC+0.1%w/vSDS, followed by one wash for 5 minutes with 200ml 0.2xSSC+0.1%w/vSDS at room temperature. This was followed by one wash for 15 minutes at 42°C with 0.2xSSC+0.1%w/vSDS, and a final rinse in 2xSSC (0.3 M NaCl, 30 mM Na₃-citrate). Membranes were then exposed to Kodak storage phosphor screens in Amersham exposure cassettes (purchased from Amersham Biosciences, Amersham, product code SO390) for a period of 24 hours. After this time the cassettes were scanned using an Amersham Molecular Dynamics Typhoon 9400 scanner to generate an image of the blot. Signals were quantified using ImageQuant software (Molecular Dynamics/GE Healthcare Life Sciences, Buckinghamshire), with background correction. Signals for *GRE2* and *CTT1* were then normalised by dividing the figure by that obtained for the *pC4/2* loading control in the same blot, to account for differences in total RNA present.

2.4.3 Radioactive labelling of DNA probes

DNA probes were used in this study to hybridise to *pC4/2*, *CTT1* and *GRE2*, with *PC4/2* acting as a loading control. The *pC4/2* probe has previously been described in the literature (Schröder et al., 2000). Probes for *GRE2* and *CTT1* were taken from stocks in the Schroeder laboratory, which had been constructed using primers detailed in Table 2. Probes were labelled with [α -³²P]-dCTP, 3000 Ci/mmol, ~10 µCi/µl. Labelling was

carried out using Rediprime II DNA labelling systems purchased from GE Healthcare life sciences, Buckinghamshire, according to manufacturer's instructions.

2.5 Chromatin Immunoprecipitation-quantitative PCR (ChIP-qPCR)

2.5.1 Chromatin Cross-Linking and Immunoprecipitation

The protocol used for chromatin immunoprecipitation was previously employed by a doctoral student in the Schroder laboratory (Siddharth Narayanan, Unpublished) and is based on an adapted version of a previously described protocol (Ren et al., 2000). Cell cultures were grown and treated as described in Chapter 2.2. Formaldehyde then added to 1% w/v, and cultures incubated for 15min at room temperature with gentle swirling to cross-link DNA. Formaldehyde then quenched by adding glycine to 125mM from a 2.5M stock. Cells were then pelleted by centrifugation for 2 mins at 3750g, and washed twice with 25ml ice-cold PBS (8.0 g/l NaCl, 0.2 g/l KCl, 14.4 g/l Na₂HPO₄, 0.2 g/l KH₂PO₄).

Cells were resuspended in 350µL ChIP Lysis buffer (50 mM HEPES·KOH, (pH 7.5), 500 mM NaCl, 1 mM EDTA, 1.0 % (v/v) Triton X-100, 0.1% (v/v) SDS, 0.1% (w/v) sodium deoxycholate), transferred to 2ml microcentrifuge tubes and 100µg 0.5mm glass beads were added. Cells were then lysed using the Precellys 24 instrument at 4°C, with 2 30-second cycles of 6500rpm and a 15-second break. The glass beads were then removed and the samples were centrifuged for 15min at 12,000g, 4°C. The supernatant from this step was discarded to remove non-crosslinked proteins and DNA. The pellets were resuspended in 350µL ChIP lysis buffer were then sonicated using a Diagenode Bioruptor as follows: 25 cycles of 15 seconds on and 30 seconds off

on high setting. This was carried out at 4°C, and samples were held in an ice-H₂O bath to prevent over-heating. Samples were then centrifuged for 30 min at 12000g, 4°C, and the pellet was discarded.

For each immunoprecipitation, 70µL of chromatin was added to 20µL of a 50% mix of Protein A-Agarose beads, and CHIP lysis buffer. Samples were incubated for 1 hour at 4°C with overhead rotation to pre-clear the samples. Agarose beads were then pelleted by centrifugation at 750g for 30 seconds and discarded, and samples were immunoprecipitated with 2µL of a selected antibody overnight, at 4°C with overhead rotation. Antibodies against Histone 3 (H3), Histone 3 acetylated at lysine 9 (referred to in the text as H3K9Ac) and Histone 4 acetylated at lysine 8 (referred to in the text as H4K8Ac) were used in this study. All antibodies were purchased from abcam, Cambridge and the product codes are detailed in Table 3.

Table 3 – Antibodies used in this study		
Antibody target	Antibody product code	Antibody Lot Number
H3	ab1791	GR237153-1
H3 (Acetyl K9)	ab10812	GR143846-4
H4 (Acetyl K8)	ab15823	GR198515-1

After immunoprecipitation, 20µL of a 50% mix of protein A-agarose beads (Purchased from Santa-cruz Biotechnology, Dallas, Texas), and CHIP lysis buffer was added to each sample, and incubated for 2 more hours with overhead rotation, 4°C. Agarose beads were then pelleted by centrifugation at 735g for 30 seconds, and the supernatant discarded. The beads were washed twice with CHIP lysis buffer, once with deoxycholate buffer (10 mM Tris-HCl (pH 8.0), 1 mM EDTA, 0.25 M LiCl, 0.5% (v/v) NP-

40, 0.5% (w/v) sodium deoxycholate), and once with 1xTE. Each wash step used 500µL of the given wash solution, and was 5 minutes long, with overhead rotation. All wash steps were carried out at 4°C, and cells were pelleted by centrifugation at 735g for 30 seconds between each wash step. Prior to washing with 1 x TE buffer, the cells were first rinsed for a few seconds with 1ml of 1 x TE, before being washed. Chromatin was then eluted from the beads by incubating for 10min at 65°C with 50µL CHIP Elution buffer (50 mM Tris-HCl (pH 8.0), 10 mM EDTA, 1 % (w/v) SDS), pre-warmed to 65°C. This elution was repeated once, and the eluates pooled. 100µL 1xTE and 1 µl 20 µg/µl proteinase K in 50 mM Tris·HCl (pH 8.0) added to eluates. Eluates were incubated for 3 hours at 55°C followed by 6 hours at 65°C, to reverse cross-links. DNA was extracted using 1 volume Phenol:Chloroform:Isoamylalcohol, saturated with Tris:HCl, pH8.0, and purified using a Probably a Wizard SV Gel and PCR clean-up kit (purchased from Promega UK, Southampton).

Simultaneously with the immunoprecipitation, 50µL of sonicated chromatin (post centrifugation) was taken to normalise the histone levels. This was used to normalise readings for the total H3 immunoprecipitations, and is referred to in the results as "Input Chromatin". To these samples, 150µL of CHIP Elution buffer, 200µL of TE buffer and 4µL 20mg/ml Proteinase K were added. Samples were incubated for 3 hours at 55°C followed by 6 hours at 65°C. DNA was extracted via 1 volume Phenol:Chloroform:Isoamylalcohol saturated with Tris:HCl, pH8.0. DNA was precipitated by adding 0.1 volume 3M NaOAc (PH=5.2), and 3 volume ethanol, and incubating overnight at -20°C. Pellets were collected by centrifugation for 30 min at 12,000 g, washed once with 70% EtOH and resuspended in 50-100µL TE Buffer.

2.5.2 Quantitative PCR (qPCR)

Samples prepared as described in 2.5.1 were stored at -20°C until ready for analysis via qPCR. All samples were ran in triplicates during qPCR analysis. All qPCR reactions consisted of 2 minutes at 95°C followed by 30-35 cycles of the following steps (95°C for 20 seconds, 55°C for 20 seconds, 72°C for 20 seconds).

All qPCR reactions consisted of 20µL final volume, with the following reagents unless stated otherwise:

- 2µL of sample DNA, prepared as detailed in 2.5.1.
- 0.1µL GE Sciences GoTaq Flexi polymerase
- 2.5mM MgCl₂
- 0.2mM dNTPs
- 0.25µM of each respective primer
- 4µL GE sciences colourless GoTaq flexi buffer
- 0.06X Sybr Green, dissolved in DMSO
- Volume was then made up to 20µL with H₂O

All qPCR Reactions were performed on Rotorgene 3000 or Rotorgene Q qPCR machines manufactured by Qiagen, Manchester. Reactions were carried out using the SYBR Green Protocol on the qPCR machines in the Cell Technology Suite in the Department of Biosciences, Durham University. Acquisition settings are detailed in Table 4. The sequences for the primers used in these qPCR experiments are detailed in Table 2.

Table 4 – Acquisition settings used for qPCR experiments in this study			
Name	Source	Detector	Gain
Green	470nm	510nm	5
Yellow	530nm	555nm	5
HRM	460nm	510nm	7

2.5.3 Analysis and Normalisation of ChIP-qPCR Data

Samples were precipitated as described in 2.5.1 and analysed by qPCR as described in 2.5.2. Rotorgene Q software was used for analysis, with relative quantitation of samples performed using the standard calculation for calculating comparative quantitations in Rotorgene Q software.

$$\text{Quantitation} = \text{Sample Amplification} ^{(\text{Calibrator Ct} - \text{Sample Ct})}$$

For experiments to analyse histone acetylation levels, a sample from the same strain and treatment precipitated with antibodies against total H3 were used as the calibrator.

Some further qPCR runs were then carried out to analyse total H3 signal alongside DNA not precipitated using antibodies. In these experiments, DNA obtained after precipitation with anti-H3 antibodies would be the sample, whilst the calibrator would be represented by an Input Chromatin sample (not treated with antibodies) from the same strain and treatment.

For visualisation of the data, in order to easily compare acetylation levels between samples before and after treatment, the figure obtained for H3K9Ac in the untreated

WT was set to 1, and all other samples from the same experiment were expressed relative to this figure.

Chapter 3 – Requirement for Rpd3L and Rpd3S complexes in transcriptional responses to osmotic stress

RPD3 is well established to be required in the transcriptional response to osmotic stress in *S. cerevisiae* (De Nadal et al., 2004, Mas et al., 2009), but which *RPD3* complex acts in this process has not been established. Findings in the literature have established that the Rpd3L complex is required for full transcriptional responses to heat shock and oxidative stress, whilst Rpd3S is dispensable (Alejandro-Osario et al., 2009, Ruiz-Roig et al., 2010). Strains deleted for Rpd3L subunits (*rpd3LΔ* strains) have also been found to have heightened sensitivity to osmotic stress (Saito and Posas, 2012). Thus, it was proposed that Rpd3L would also be required for the response to osmotic stress, whilst Rpd3S would be dispensable in this process. The view that this is most likely has also been proposed in the literature (Saito and Posas, 2012). Northern blotting as described in Chapter 2.4 was carried out to analyse how the transcriptional responses of *S. cerevisiae* to osmotic stress induced by NaCl and sorbitol were affected by loss of Rpd3L and Rpd3S subunits.

3.1 *rpd3LΔ* mutants show defect in the transcriptional response to NaCl-induced osmotic stress

Figure 5 shows the results of Northern blotting following exposure of WT and *rpd3LΔ* strains to osmotic stress induced via 0.6M NaCl and 1.2M Sorbitol. Northern blotting was carried out as discussed in Section 2.3, and the membranes were probed for *CTT1* and *GRE2*, with pC4/2 used as a loading control to normalise expression levels. As can be seen, both the *rpd3LΔ* strain and most of the various *rpd3LΔ* mutants tested show a distinct defect in the transcriptional response to osmotic stressing via 0.6M NaCl.

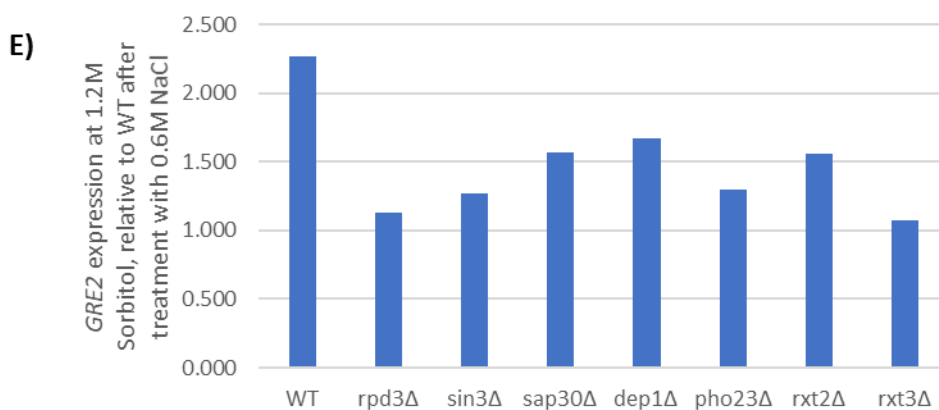
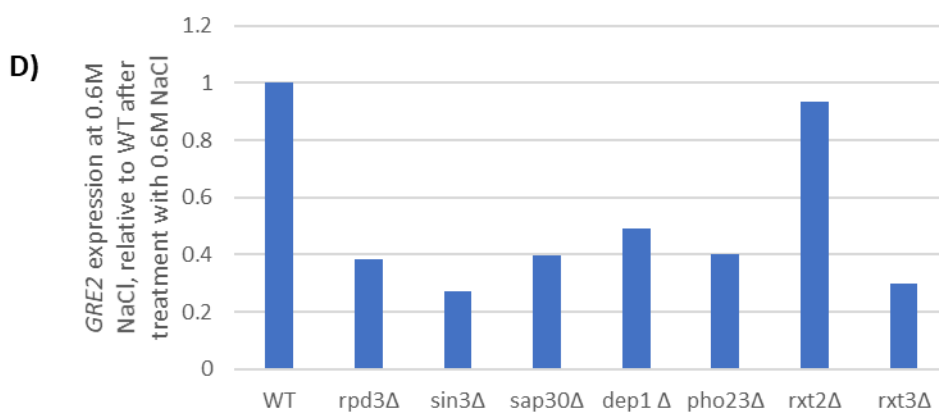
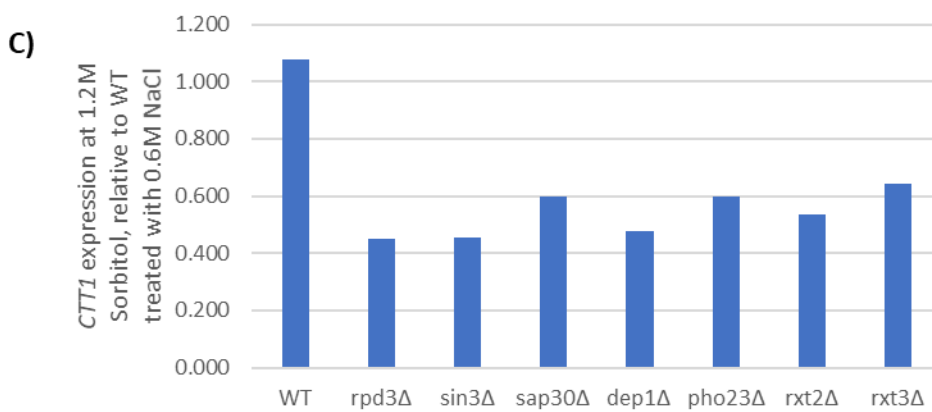
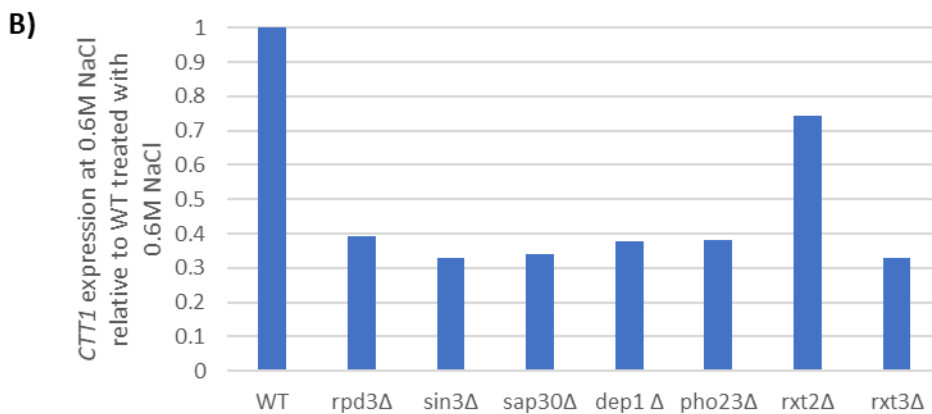
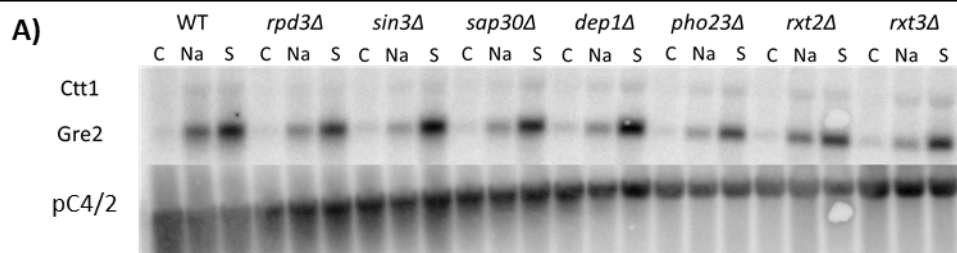


Figure 5 – Northern blot analysis of the transcriptional responses of WT and *rpd3Δ* mutants to osmotic stress via 0.6M NaCl (Na) and 1.2M sorbitol (S).

A) Image of northern blot showing expression of *Ctt1* and *Gre2* in untreated cells (labelled “C” in the diagram), and after treatment with 0.6M NaCl (Na) and 1.2M sorbitol (S) for 60 min.

B) Expression levels of *CTT1* in WT and *rpd3Δ* strains after treatment with 0.6M NaCl, relative to WT. Expression levels for each strain were normalised by division by the loading control (*pC4/2*) signal for that strain, then expressed as a proportion of the signal for WT treated with 0.6M NaCl for 60 min.

C) Expression levels of *CTT1* in WT and *rpd3Δ* strains after treatment with 1.2M sorbitol for 60 min, relative to WT treated with 0.6M NaCl for 60 min. Expression levels for each strain were normalised by division by the loading control (*pC4/2*) signal for that strain, then expressed as a proportion of the signal for WT treated with 0.6M NaCl for 60 min, such that the level of transcriptional induction by each stressing reagent could be compared in the same strain.

D) Expression levels of *GRE2* in WT and *rpd3Δ* strains after treatment with 0.6M NaCl for 60 min, relative to WT. Expression levels for each strain were normalised by division by the loading control (*pC4/2*) for that strain, then expressed as a proportion of the signal for WT treated with 0.6M NaCl for 60 min.

E) Expression levels of *GRE2* in WT and *rpd3Δ* strains after treatment with 1.2M sorbitol for 60 min, relative to WT treated with 0.6M NaCl for 60 min. Expression levels for each strain were normalised by division by the loading control (*pC4/2*) signal for that strain, then expressed as a proportion of the signal for WT treated with 0.6M NaCl for 60 min, such that the level of transcriptional induction by each stressing reagent could be compared in the same strain.

WT=MSY136-40/*rpd3Δ*=JN1/*sin3Δ*=JN2/*sap30Δ*=JN3/*dep1Δ*=JN4/*pho23Δ*=JN6/*rxt2Δ*=JN7/*rxt3Δ*=JN8

This defect is immediately apparent both upon visual analysis of the radiolabelled blot image (Figure 5A) and when visualising expression levels of the genes after normalising against a loading control (Figures 5B and 5D). All *rpd3Δ* strains show lower expression of both *CTT1* and *GRE2* after osmotic stressing than the WT exposed to the same stressing conditions. This result is in agreement with the experimental hypothesis as explained in Chapter 1. It is also consistent with both previous unpublished work in the Schroder laboratory and previous findings in the literature (Loewith et al., 2001, Alejandro-Osario et al., 2009, Ruiz-Roig et al., 2010). The only unexpected result in

these data is an unexpectedly high transcriptional response in the *rxt2Δ* mutant, with distinctly higher expression of both *CTT1* and *GRE2* than other *rpd3LΔ* mutants (Figure 5B and 5D). This finding is difficult to explain from previous observations and represents a potentially novel finding about the respective roles of the different Rpd3L subunits in the osmotic stress response.

Further repeats utilising the same NaCl stressing conditions (0.6M NaCl for 60 mins) were carried out to increase confidence in the data observed and provide robust evidence that *rpd3LΔ* mutants are defective in the transcriptional response to osmotic stress. A further repeat shown in Figure 6 also displays a general defect in transcriptional response to 0.6M NaCl-induced osmotic stress in *rpd3LΔ* strains, with all except 1 strains showing reduced expression of both *CTT1* and *GRE2* than WT after treatment with 0.6M NaCl (Figure 6B and Figure 6D). *rxt2Δ* again shows an increased expression level relative to *rpd3Δ*, whilst still being lower than WT (Figure 6B and 6D), a feature also apparent in Figure 5B and 5D. This is consistent with the findings in the previous repeat (Figure 5) and this consistency merits further investigation into the transcriptional responses of *rxt2Δ* strains to osmotic stress.

Despite the general defect in transcriptional responses in *rpd3LΔ*, this repeat also shows several unexpected results, with *cti6Δ* actually showing higher expression (albeit marginally) of both *CTT1* and *GRE2* than WT after treatment with 0.6M NaCl (Figure 6B and 6D). *sin3Δ* and *pho23Δ* also show far higher expression of both genes tested than *rpd3Δ* after osmotic stress (Figures 6B and 6D), although their expression level is lower than WT. These are unexpected findings, and do not agree with the experimental hypotheses based on previous literature observations or the data for the previous

repeat shown in Figure 5 (although *cti6Δ* was not tested in this repeat). There are several reasons apparent in Figure 6A highlighting technical challenges that may help explain these unexpected results. Firstly, it is immediately apparent that the hybridisation signals are much fainter than those for Figure 5. This likely indicates an issue with either cross-linking of RNA to the membrane, or with the efficiency of the probe labelling method, which may introduce error into the readings. Secondly, it is apparent that degradation may have occurred in RNA from the WT strain during the RNA extraction procedure (Figure 6A), which may adversely affect the measurements for expression in this strain. In light of these features, it is logical to suggest that Figure 5 is more likely to indicate biologically accurate data, meaning the discrepancies observed in Figure 6 are more likely to represent experimental error.

Overall, we can conclude that the data obtained do display defect in *rpd3LΔ* mutants in the transcriptional response to osmotic stress, at least at the *GRE2* and *CTT1* Loci. This finding is consistent with previous literature findings (Loewith et al., 2001, Alejandro-Osario et al., 2009, Ruiz Roig et al., 2010) and the experimental hypotheses outlined in Chapter 1. We can also note that *rxl2Δ* consistently displays a stronger response than most *rpd3LΔ* mutants, which would be a novel finding potentially suggestive of a reduced requirement for *rxl2Δ* in this process and worthy of further investigation. However, multiple repeats of the quality observed in Figure 5 are required to assert these findings with confidence, which time pressures did not allow during this project. Further repeats are also required to conclude whether the higher-than-expected expression levels observed in Figure 6 for *sin3Δ*, *cti6Δ* and *pho23Δ* are in fact

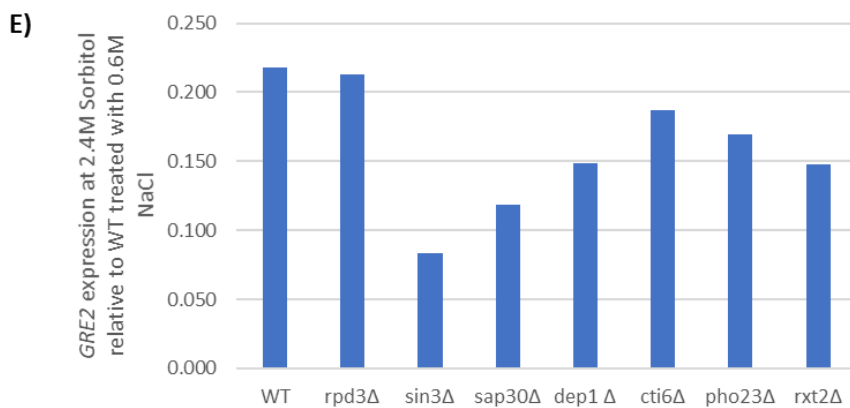
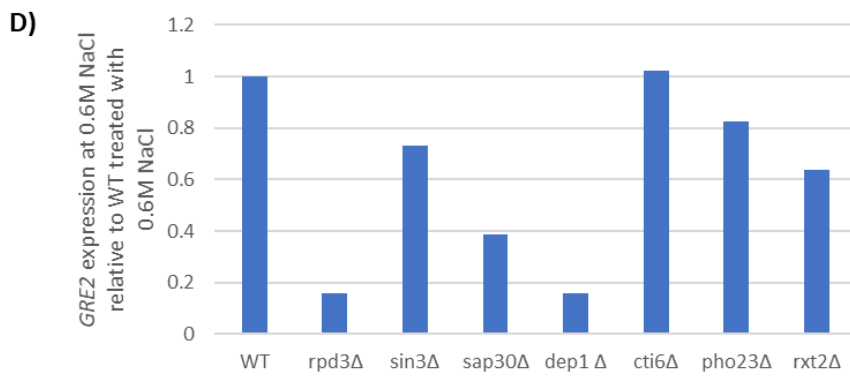
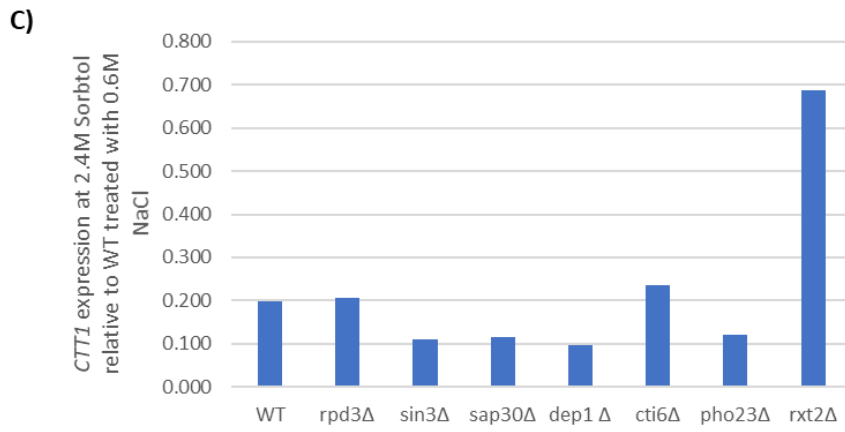
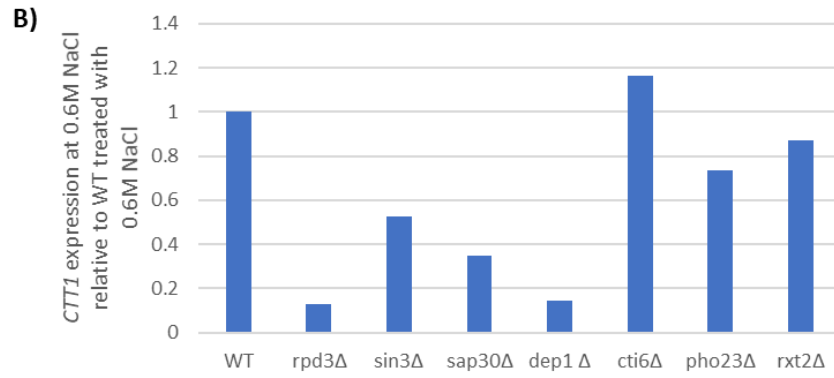
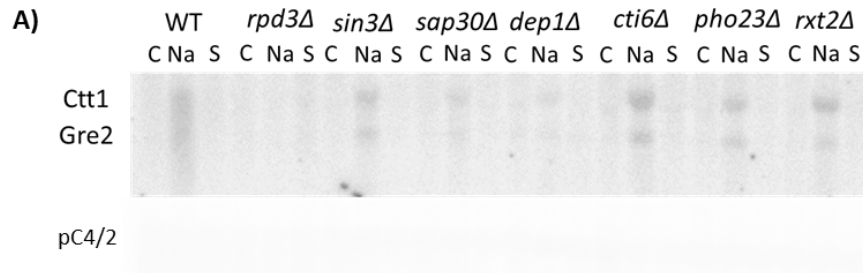


Figure 6 – Northern blot analysis of the transcriptional responses of WT and *rpd3Δ* mutants to osmotic stress via 0.6M NaCl (Na) and 2.4M Sorbitol (S).

A) Image of northern blot showing expression of *Ctt1* and *Gre2* in untreated cells (C) and after exposure to 0.6M NaCl (Na) and 2.4M sorbitol (S) for 60 minutes, and loading control *pC4/2*. B) Expression levels of *CTT1* in WT and *rpd3Δ* strains after treatment with 0.6M NaCl for 60 min, relative to WT. Expression levels for each strain were normalised by division by the loading control (*pC4/2*) signal for that strain, then expressed as a proportion of the signal for WT treated with 0.6M NaCl for 60 min. C) Expression levels of *CTT1* in WT and *rpd3Δ* strains after treatment with 2.4M sorbitol for 60 min, relative to WT treated with 0.6M NaCl for 60 min. Expression levels for each strain were normalised by division by the loading control (*pC4/2*) signal for that strain, then expressed as a proportion of the signal for WT treated with 0.6M NaCl for 60 min, such that the level of transcriptional induction by each stressing reagent could be compared in the same strain. D) Expression levels of *GRE2* in WT and *rpd3Δ* strains after treatment with 0.6M NaCl for 60 min, relative to WT. Expression levels for each strain were normalised by division by the loading control (*pC4/2*) signal for that strain, then expressed as a proportion of the signal for WT treated with 0.6M NaCl for 60 min. E) Expression levels of *GRE2* in WT and *rpd3Δ* strains after treatment with 2.4M sorbitol, relative to WT treated with 0.6M NaCl for 60 min. Expression levels for each strain were normalised by division by the loading control (*pC4/2*) signal for that strain, then expressed as a proportion of the signal for WT treated with 0.6M NaCl for 60 min, such that the level of transcriptional induction by each stressing reagent could be compared in the same strain.

WT=MSY13640/*rpd3Δ*=JN1/*sin3Δ*=JN2/*sap30Δ*=JN3/*dep1Δ*=JN4/
cti6Δ=JN5/*pho23Δ*=JN6/*rxt2Δ*=JN7

experimental error as suggested earlier, or indicative of biological variation. This would be a priority for further work in the area.

3.2 No evidence of a defect in transcriptional responses to NaCl-induced osmotic stress was found in *rpd3Δ* strains

Northern blotting was also carried out to analyse the transcriptional responses of *rpd3Δ* strains to NaCl-induced osmotic stress. WT, *rpd3Δ* and *rpd3Δ* strains were

exposed to 0.6M NaCl for 60 mins, with RNA extraction and northern blotting carried out as described in 2.4, with membranes probed for expression levels of *CTT1* and *GRE2* (Figure 7). Previous results in the literature have found Rpd3S subunits to be dispensable for transcriptional responses to heat shock and oxidative stress (Loewith et al 2001; Ruiz-Roig et al 2012; Alejandro-Osario et al 2009). We thus hypothesised that the same results would be found for the osmotic stress response, which does seem apparent upon visual examination of the blot in Figure 7(A). *rpd3Δ* and *sin3Δ* strains (essential subunits of both the Rpd3L and Rpd3S complexes) appear to have less expression than WT strains after treatment with 0.6M NaCl for 60 mins (Figure 7A). This is particularly apparent for *rpd3Δ*. Meanwhile, strains carrying deletions in Rpd3S-specific subunits *RCO1* and *EAF3* seem to have expression levels similar to, or higher than, the WT, particularly at the *CTT1* locus. These observations are consistent with the experimental hypotheses and previous literature observations as discussed.

However, this blot also encountered technical issues, making it difficult to draw robust conclusions from this data. The bands are very faint, similar to those in Figure 6, suggesting problems with hybridisation or cross-linking of the RNA to the membrane. Additionally, and much more significantly is the issue that the quantifications of gene expression normalised against *pC4/2* in Figure 7(B-E) do not appear to match the relative expression levels as determined by a visual analysis of the blot in Figure 7(A). The expression levels of the strains after treatment with 0.6M NaCl for 60 mins (Figure 7B and 7D) do indicate a higher expression of *CTT1* in *rpd35Δ* strains than *rpd3Δ*, but only marginally. *GRE2* expression after 0.6M NaCl exposure (Figure 7D) shows even more discrepancy, and in particular, the *GRE2* expression for the *eaf3Δ* strain (Figure 7D) does not appear to match the bands present in the blot in Figure 7(A). This could indicate that

the membrane was damaged or otherwise compromised between the hybridisation against *CTT1* and *GRE2*, and the later hybridisation against *pC4/2* as a loading control,

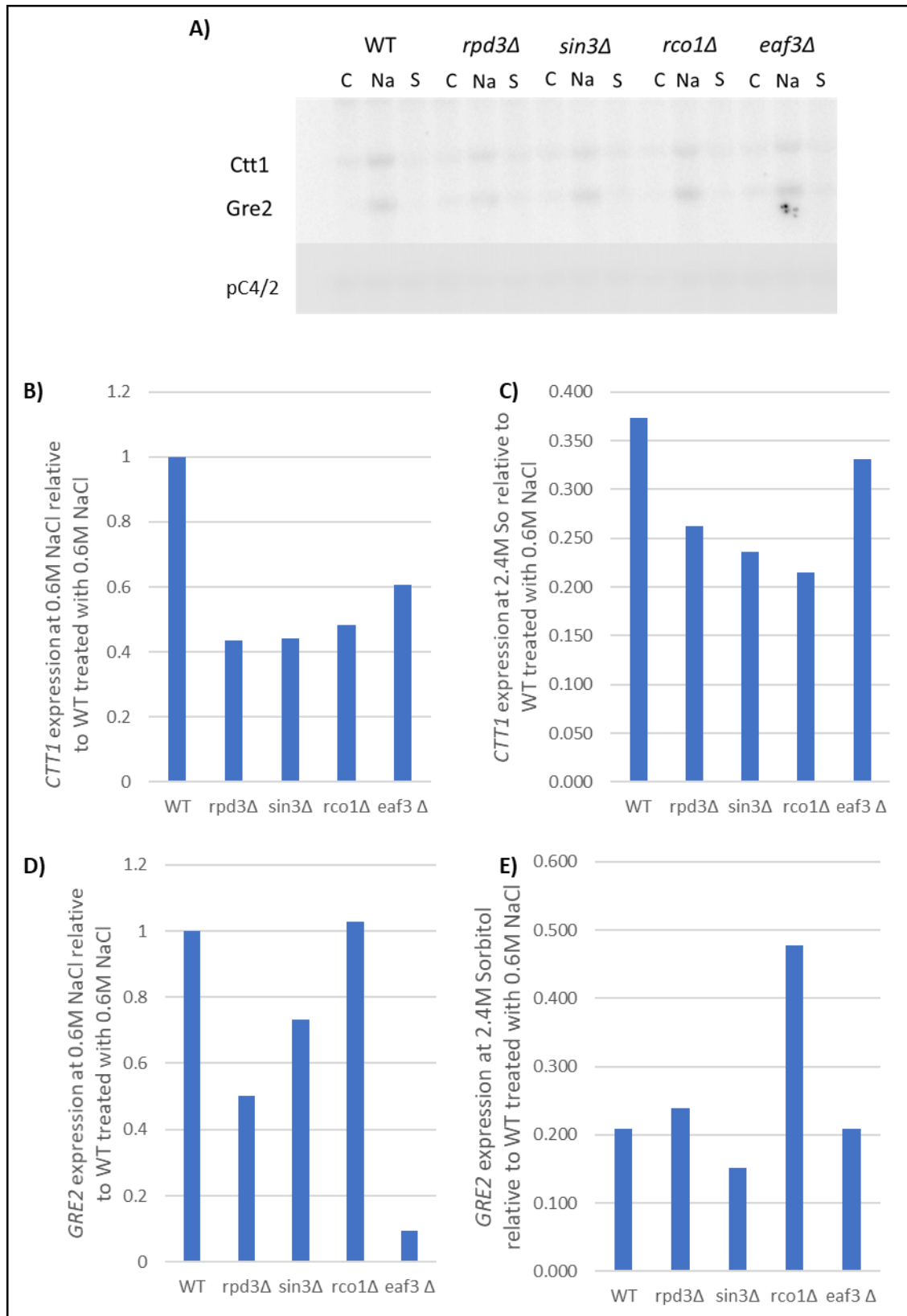


Figure 7 – Northern blot analysis of the transcriptional responses of WT and *rpd35Δ* mutants to osmotic stress via 0.6M NaCl and 2.4M Sorbitol.

A) Image of northern blot showing expression of *Ctt1* and *Gre2* in untreated cells (C) and after exposure to 0.6M NaCl (Na) and 2.4M Sorbitol (S) for 60 minutes. B) Expression levels of *CTT1* in WT and *rpd35Δ* strains after treatment with 0.6M NaCl for 60 min, relative to WT. Expression levels for each gene were normalised by dividing by the loading control (*pC4/2*) signal for that strain, and then expressed as a proportion of the signal for WT treated with 0.6M NaCl for 60 min. C) Expression levels of *GRE2* in WT and *rpd35Δ* strains after treatment with 2.4M sorbitol for 60 min, relative to WT. Expression levels for each gene were normalised by dividing by the loading control (*pC4/2*) signal for that strain, and then expressed as a proportion of the signal for WT treated with 0.6M NaCl for 60 min. D) Expression levels of *GRE2* in WT and *rpd35Δ* strains after treatment with 0.6M NaCl for 60 min, relative to WT. Expression levels for each gene were normalised by dividing by the loading control (*pC4/2*) signal for that strain, and then expressed as a proportion of the signal for WT treated with 0.6M NaCl for 60 min. E) Expression levels of *GRE2* in WT and *rpd35Δ* strains after treatment with 2.4M sorbitol for 60 min, relative to WT. Expression levels for each gene were normalised by dividing by the loading control (*pC4/2*) signal for that strain, and then expressed as a proportion of the signal for WT treated with 0.6M NaCl for 60 min.

WT=MSY134-36/*rpd3Δ*=JN9/*sin3Δ*=JN10/*rco1Δ*=JN11/*eaf3Δ*=JN12

resulting in inappropriate normalisation and a distortion of the expression readings. Alternatively, it could be that there are distinct differences in quantity of RNA loaded in the blot, and that the bands in Figure 7(A) are an experimental artefact that do not show the true picture of relative gene expression in these mutants. The faint bands compound this problem, as the loading controls are particularly faint and difficult to analyse visually. These factors suggest that this data may be erroneous and not accurately representative of the transcriptional responses of these strains, limiting confidence in these data. Thus, robust conclusions are difficult to draw with regards to the behaviour of *rpd35Δ* strains after NaCl-induced osmotic stress, and further repeats of these blots would be needed. However, visual analysis of the blot in Figure 7(A) does suggest that

rco1Δ and *ef3Δ* do not have a striking defect in the transcriptional response to NaCl-induced osmotic stress.

3.3 Investigation of sorbitol stress responses and optimisation of stressing conditions

The Northern blots displayed in Figures 5 and 6 also analysed transcriptional responses to sorbitol (1.2M and 2.4M respectively). Although the blot in Figure 5A does not suggest a defect in transcriptional responses to 1.2M sorbitol in the *rpd3Δ* strains, analysis of relative expression after normalisation against the loading control (Figure 5C and 5E) does show a strong and consistent defect. All of the *rpd3Δ* strains show distinctly reduced expression of both *CTT1* and *GRE2* in response to 1.2M sorbitol relative to WT, in keeping with experimental predictions based on prior literature observations. Thus, *rpd3Δ* strains also seem to be defective in their transcriptional response to 1.2M sorbitol, as well as the response to 0.6M NaCl. This finding is important as it highlights consistency in the transcriptional responses of the strains to two independent osmotic stressing conditions. Alongside osmotic stress, NaCl also induces ionic stress, by affecting the extracellular concentration of Na⁺ ions. Thus, it could be that NaCl has effects on transcription in *S. cerevisiae* outside of the osmotic stress response. The identification of defects in response to 1.2M sorbitol thus heightens confidence that the differences observed reflect defects in the osmotic stress response in *S. cerevisiae*.

However, lack of visually observably weaker signals in the blot mean that these results are not ideal for providing conclusive evidence of a transcriptional defect. It was considered that perhaps the conditions of exposure to sorbitol selected (1.2M for 60 minutes) may be non-optimal for full observation of a transcriptional defect, if present.

Transcriptional responses to osmotic stress show an initial increase, followed by a gradual decrease in stress-responsive gene expression (Dolz-Edo et al., 2013). *rpd3Δ* strains show a delay in transcriptional responses, so if the time point selected was after the peak in response for the WT strains used, it may bias the results in favour of the *rpd3Δ* and *rpd3LΔ* strains. It is also worth noting that the expression levels of both *CTT1* and *GRE2* are higher for all strains after exposure to 1.2M sorbitol (Figure 5C and 5E respectively) than they are for the same strain after exposure to 0.6M NaCl (Figure 5B and 5D), with the exception of *CTT1* expression in *rxt2Δ*. It could be that these higher signals make it more difficult to observe transcriptional defects visually, as strong signals are present even in strains which did not undergo full transcriptional responses. To solve this issue, the concentration of sorbitol was increased.

Transcriptional stress responses are delayed and reduced by a higher dosage of osmotic stress (Dolz-Edo et al., 2013), so I hypothesised that increasing the sorbitol concentration may allow us to observe a defect in the *rpd3LΔ* strains.

The results of this approach are shown in Figure 6 (for *rpd3LΔ* strains) and Figure 7 (for *rpd3SΔ* strains). The gene expression levels are shown relative to the WT strain after treatment with 0.6M NaCl, to allow comparison of transcriptional responses to the 2 stressing reagents. Virtually no induction of *CTT1* or *GRE2* was observed in response to 2.4M sorbitol after 60 mins in any strains, including WT (Figure 6C and 6E) (Figure 7C and 7E). The only similar transcriptional induction observed after exposure to 2.4M sorbitol, relative to 0.6M NaCl, is the *rxt2* strain, which shows an expression level at *CTT1* ~70% of that seen in the WT after 0.6M NaCl treatment (Figure 5C). *rco1Δ* also shows *GRE2* expression ~50% of that observed in the WT after stressing with 0.6M

NaCl. In all other cases, expression levels after 2.4M sorbitol treatment are around 35% of those seen in WT strains after 0.6M NaCl treatment or lower (Figure 5C and 5E) (Figure 7C and 7E). These low expression levels mean it is difficult to analyse the blots or draw robust conclusions from this data with regards to transcriptional responses to 2.4M sorbitol. In light of these poor results it was apparent that more investigation and optimisation of this procedure was required in order to obtain informative data.

It was decided to carry out dose response curves for *CTT1* and *GRE2* under sorbitol-induced osmotic stress, to investigate the nature of the transcriptional response and identify the optimum conditions for inducing a maximal transcriptional response in the WT. Once this was optimised, *rpd3Δ* mutants could then be stressed under these conditions, to identify conditions where *rpd3Δ* were observably defective in the response. *rpd3LΔ* and *rpd3SΔ* strains could then be tested to see if the transcriptional defect was conserved among different Rpd3L subunits.

WT strain was exposed to a range of sorbitol concentrations, from 0.6M to 2.4M, and for a range of times, from 30 mins to 240 mins (Figure 8A). The transcriptional response was strongest at 30min for 0.6M and 1.2M, increasing to 60-120 mins for 1.8M (Figure 8A). Little transcriptional response is observed to 2.4M sorbitol even at 240 mins, explaining the poor induction previously observed in the northern blots using 2.4M for 60 mins (Figures 6 and 7).

WT and *rpd3Δ* strains were then exposed to the two concentrations to which WT showed the strongest response (1.2M and 1.8M), for periods of time ranging from 30 mins to 120 mins (Figure 8B). A delay in the transcriptional response to both concentrations is apparent in *rpd3Δ* strain compared to WT. Using these data,

treatment conditions could be selected where WT shows a strong transcriptional response but *rpd3Δ* does not, with 1.2M Sorbitol for 30 min and 1.8M Sorbitol for 90-120 min the most obvious candidates (Figure 8B). Exposure to 1.2M sorbitol for 30 minutes was selected as the optimum stressing conditions for observing a transcriptional defect in *rpd3Δ* and strains deleted for individual complex subunits. Producing good quality blots of the deletion strains analysed in this report under these stressing conditions would be a priority of further work in this area.

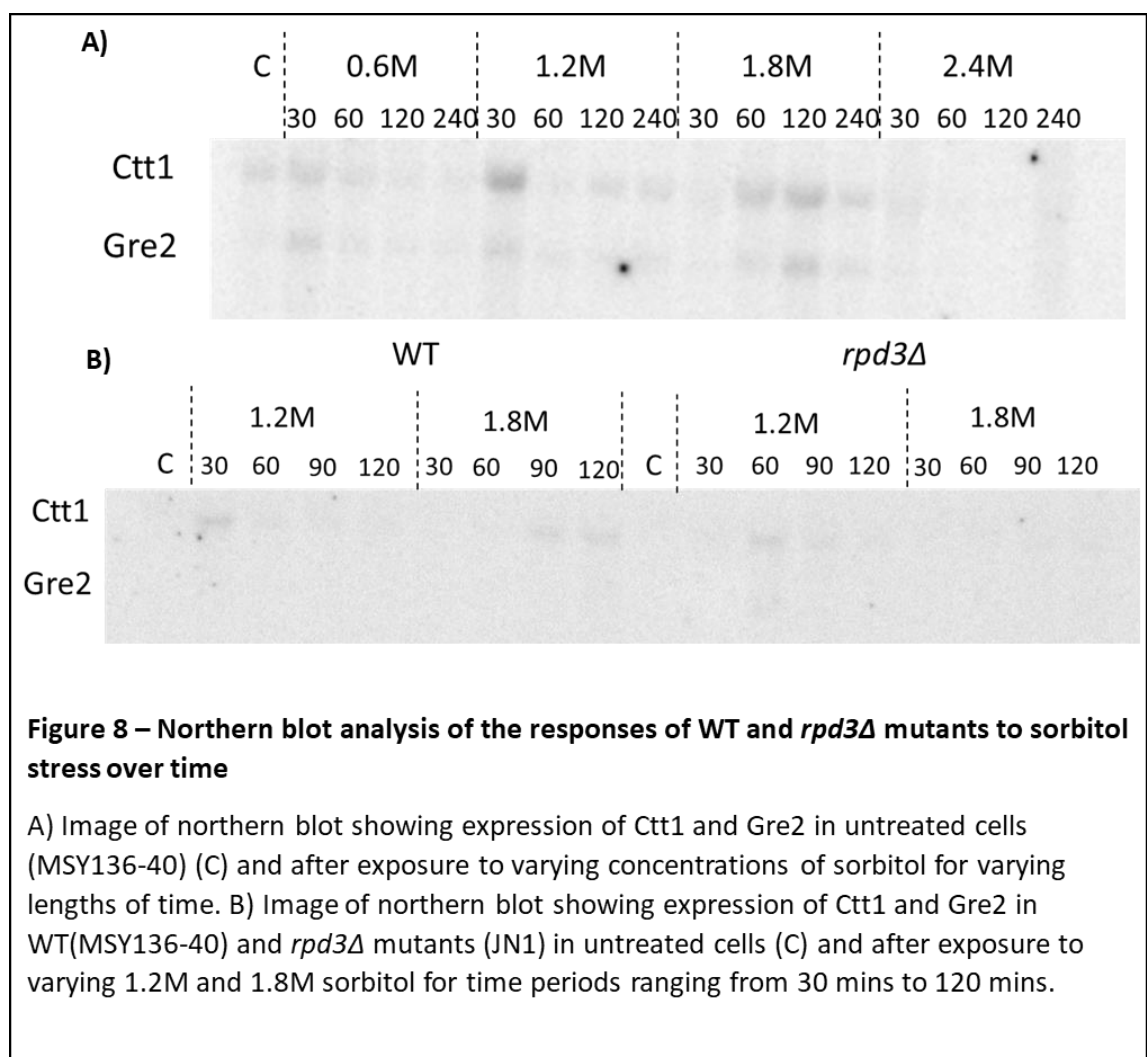


Figure 8 – Northern blot analysis of the responses of WT and *rpd3Δ* mutants to sorbitol stress over time

A) Image of northern blot showing expression of Ctt1 and Gre2 in untreated cells (MSY136-40) (C) and after exposure to varying concentrations of sorbitol for varying lengths of time. B) Image of northern blot showing expression of Ctt1 and Gre2 in WT (MSY136-40) and *rpd3Δ* mutants (JN1) in untreated cells (C) and after exposure to varying 1.2M and 1.8M sorbitol for time periods ranging from 30 mins to 120 mins.

3.4 Summary and Discussion of Northern Blotting analysis

Significant technical challenges were encountered with the northern blotting experiments, with only one blot producing high quality data (Figure 5). The other blots shown in Figures 6 and 7 are compromised by degradation (Figure 6), faint bands (particularly for loading controls) and in some cases expression level data which does not seem to match to the blot in question (Figure 7). The faint bands in particular suggest a problem with the hybridisation or probe labelling protocols. Several possible reasons for these challenges were investigated and discounted. Fresh DNA probes for radiolabelling were made from concentrated stocks in the Schroder laboratory, to account for any possible degradation in the working solutions used and verified to be the optimal concentration of 10ng/ μ l. The probes were also verified to be the correct product size via gel electrophoresis. The radiolabelling procedure was repeated under supervision, to check for errors in this procedure. Finally, an attempt was made to test an attempt was made to check the specific activity of the radiolabelled probes, using methodology outlined in (Sambrook et al., 1989) but this was unsuccessful. It was also considered whether the UV cross-linker may have been inaccurate, resulting in faulty cross-linking of RNA to membranes. However, further work in the Schroeder laboratory (unpublished) has suggested the cross-linker is still functional. The only other apparent explanation for these failures is that mistakes were made in handling the DNA probes after denaturation, and that the DNA probes may have renatured with each other prior to hybridisation with the RNA on the membrane. Investigating and fixing this problem would be an immediate priority for further work in this area.

The technical challenges encountered place limits on the conclusions that can be drawn from the data. The issues encountered with loading controls are particularly problematic. Figures 6 and 7 have bands for pC4/2 loading controls which are faint to the point of being almost unreadable. This raises serious questions about the validity of the normalisation, and thus the quantitation of the expression levels presented. Furthermore, even Figure 5, the highest quality data, exhibits high variation in the amount of total RNA loaded, as evidenced by the variation in the bands for pC4/2 in Figure 5(A). This variation means the data can be potentially misleading, as a visual examination of the blot does not present the same conclusions as an examination of the normalised quantitative gene expression data presented in Figure 5 (B) – (E). A final problem stemming from these technical challenges is that it prevented statistical analysis from being carried out. Due to the issues encountered, it was not possible to obtain three blots analysing the transcriptional responses of any one set of mutants, meaning that T-tests to analyse the statistical significance of any differences in expression between strains could not be performed. Equally, it was not possible to apply standard deviation or error to the quantified expression levels.

The technical challenges encountered mean that this data is not sufficient to confidently present new findings to the field regarding the role of Rpd3 in transcriptional responses to osmotic stress. However, some trends can be observed in the data, particularly with regard to *rpd3 Δ* deletion mutants, which display a defect in the transcriptional response to osmotic stress, compared to WT (Figures 5 and 6). The defect occurs consistently under 2 different osmotic stress regimes (0.6M NaCl and 1.2M sorbitol, both for 60 mins), increasing confidence that this defect is related to the osmotic stress response, rather than other NaCl-specific transcriptional responses. This

defect does not seem apparent in *rpd35Δ* strains (*rco1Δ* and *eaf3Δ*) although this data is less clear and this conclusion not as robust.

Chapter 4 - ChIP-qPCR Analysis of histone acetylation and occupancy during the osmotic stress response

The reported function of *RPD3* in activating transcription was unexpected as it contradicts the canonical role of histone deacetylases as transcriptional repressors. However, the question as to whether genetic loci regulated by *RPD3* undergo an increase or decrease in acetylation during transcriptional activation has not yet been definitively answered. This is a major requisite if we are to understand the mechanisms of *RPD3*-regulated gene expression, and has the potential to help inform our understanding of other patterns of histone modifications and their relation to transcriptional activity. As discussed in Chapter 1.3.1 the findings of (De Nadal et al., 2004) observed deacetylation alongside transcriptional induction, but a contrasting finding was observed in (Magraner-Pardo et al., 2014), with differences in normalisation perhaps being a major factor behind the disagreement. A previous analysis of the relationship between nucleosome occupancy and transcriptional activation offers strong reasoning for taking this factor into account when calibrating data from chromatin immunoprecipitation (Poklohok et al., 2005). Previous work in the Schroder laboratory has largely concurred with that of (Magraner-Pardo et al., 2014), finding an increase in acetylation and loss of histones concurrently with transcriptional activation during osmostress. This has previously been found to be the case with osmostress responses in mammalian cells (Tong et al., 2009). It is also important to discover whether changes in acetylation and histone occupancy correlate with transcriptional activation when strains carrying deletions in different *RPD3* complexes are analysed. If differences in acetylation are found in the same strains as differences in transcriptional responses it

would be consistent with these histone modifications playing a mechanistic role in the transcriptional initiation process.

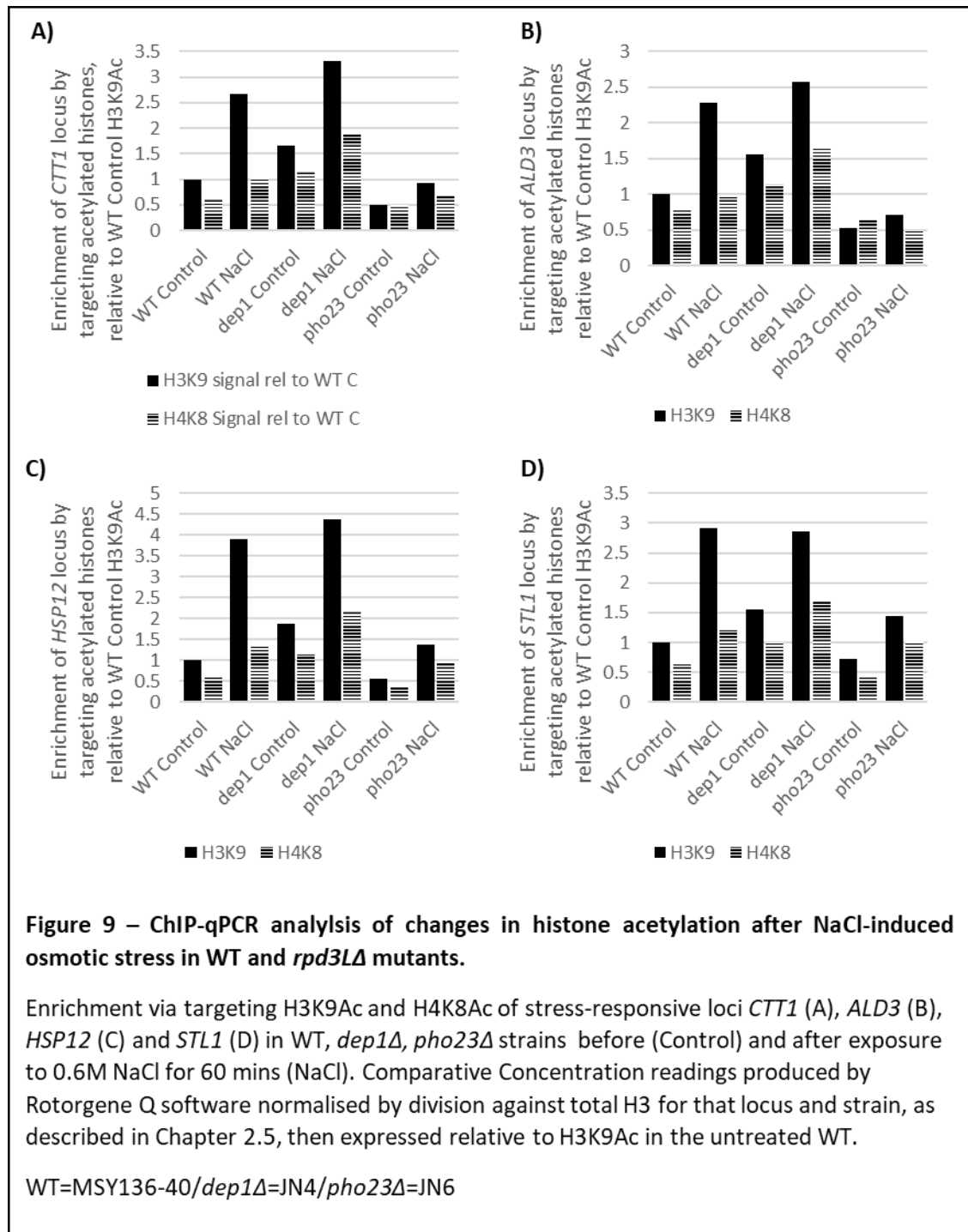
4.1 *rpd3 Δ* strains display defect in acetylation and histone loss at stress-induced loci after osmotic stress

Following analysis of Figure 5, which indicated a defect in transcriptional responses to 0.6M NaCl after 60 minutes in *rpd3 Δ* strains, investigations were made into changes in acetylation under these stressing conditions in *rpd3 Δ* strains. Chromatin immunoprecipitation followed by quantitative PCR was carried out as discussed in Chapter 2.5, analysing enrichment of certain gene loci via precipitation with antibodies targeting histones acetylated at H3K9 (H3K9Ac) and H4K8 (H4K8Ac), with total H3 levels used to normalise the data as described in Chapter 1.3.1. *CTT1*, *ALD3*, *STL1* and *HSP12* were selected for analysis as they are known to be upregulated in response to osmotic stress known to be transcriptionally upregulated in response to osmotic stress and have been cited as regulated by Rpd3 activity (De Nadal et al., 2004). These genes were analysed in WT, *dep1 Δ* and *pho23 Δ* strains (both of which are Rpd3L subunits). Based on previous work in the Schroder laboratory (unpublished) and (Magraner-Pardo et al., 2014), it was hypothesised that acetylation and histone loss would occur in the WT, and that these would be defective in *rpd3 Δ* strains. The WT strain showed a strong increase (at least 2-fold) in H3K9Ac at all gene loci (Figure 9). The relative increase in acetylation (Treated/Untreated) after osmotic stressing is smaller in both *rpd3 Δ* mutants at all 4 gene loci, relative to that observed in the WT strain at the same gene locus (Figure 9). This is consistent with the experimental hypotheses. Meanwhile acetylation at H4K8 shows more variation. WT and *dep1 Δ* strains still show an increase in acetylation at this

position, but markedly reduced compared to that observed at H3K9 (Figure 9) whilst the *pho23Δ* strain is observed to show both increased and decreased acetylation at different gene loci. Previous findings in the literature may explain the different dynamics at these two loci in the osmotic stress response. The authors of (Magraner-Pardo et al., 2014) found H3K9 acetylation to be linked to transcriptional upregulation, but found that change at H4K8 had little effect. It was also discussed how acetylation at H3K9 and H4K8 are catalysed by different chromatin modifiers (Magraner-Pardo et al., 2014). Thus, it can be proposed that H3K9 acetylation is delicately regulated during this process to coordinate transcriptional responses, and thus would be expected to be consistent in transcriptionally competent cells, and consistently defective in transcriptionally-defective cells. H4K8, meanwhile, may not be under such tight control during this stress response, and may be more open to stochastic fluctuation. These observations are consistent with the hypothesis that *RPD3* is required for site-specific changes in acetylation, and that this mechanistically linked to transcriptional responses (and thus absent in strains defective for transcriptional initiation).

In addition, total H3 levels were also tested, with Input Chromatin used to normalise the data as discussed in section 2.5. Again, the data fits with our expected hypotheses, with the WT strain showing a notable decrease in total H3 at all 4 genomic loci tested (Figure 10). *dep1Δ* also shows decrease in total H3 but to a reduced extent, whilst *Pho23Δ* shows increase in total H3 levels after osmotic stress at some genes. This data correlates with the findings of (Magraner-Pardo et al., 2014) and helps explain some differences between this report and the findings of (De Nadal et al., 2004). The authors of (De Nadal et al., 2004) normalised their ChIP-qPCR data against telomeres, and did not consider total histone occupancy at the genomic locations they analysed. Thus, a large decrease

in total H3 may have led them to erroneously conclude that deacetylation was occurring. It is also notable that *pho23Δ* shows the largest deviation from the WT in these experiments. *dep1Δ* seems to behave like WT but to a markedly reduced extent, whilst *pho23Δ* undergoes a different pattern of activity, with both acetylation levels and total H3 occupancy moving in the opposite direction to WT at certain loci (Figure 9).



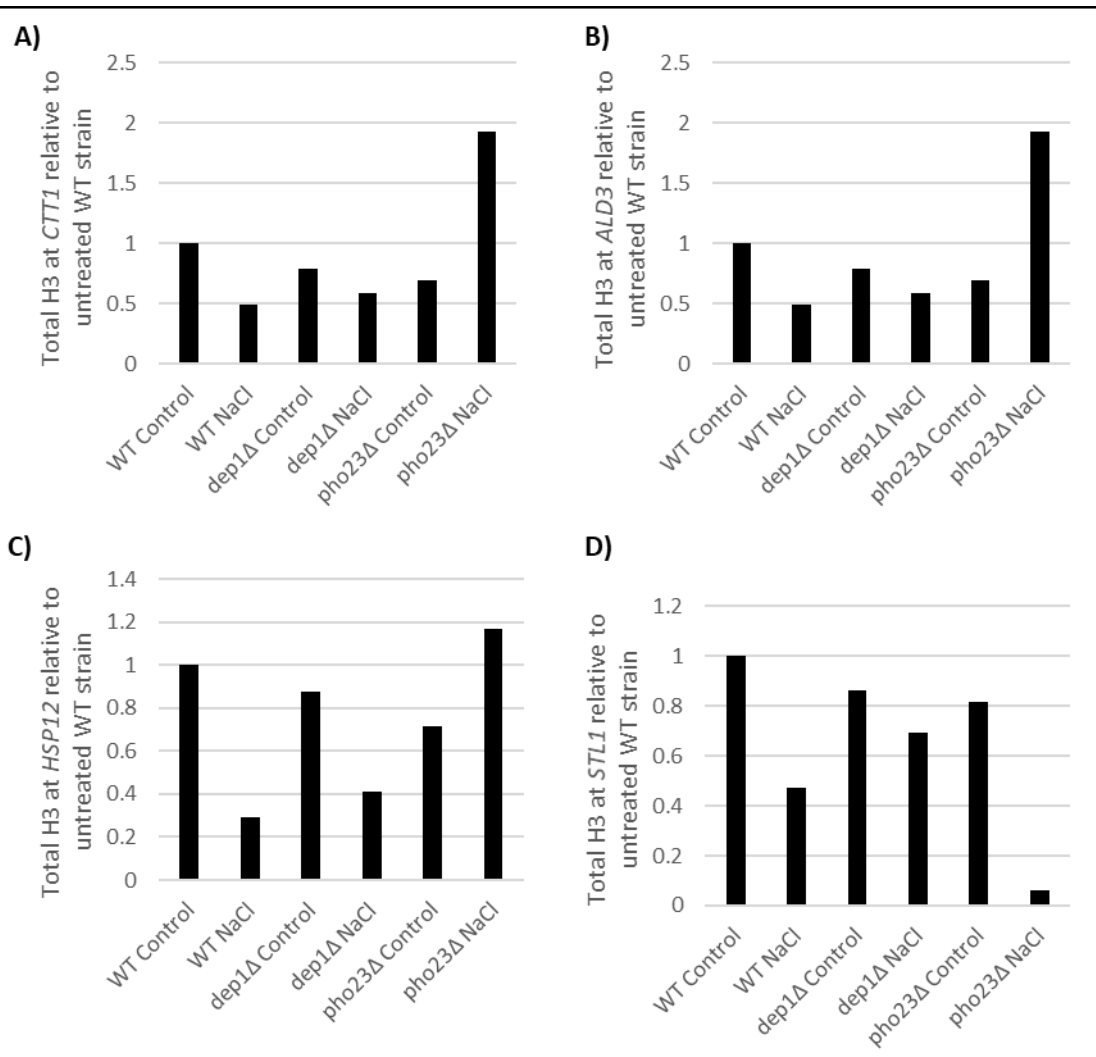


Figure 10 – ChIP-qPCR analysis of changes in H3 occupancy after NaCl-induced osmotic stress in WT and *rpd3Δ* mutants.

Total H3 levels at stress-responsive loci *CTT1* (A), *ALD3* (B), *HSP12* (C) and *STL1* (D) in WT, *dep1Δ*, *pho23Δ* strains before (Control) and after exposure to 0.6M NaCl for 60 mins (NaCl). Comparative Concentration readings were produced by Rotorgene Q software were normalised by division against Input Chromatin for that locus and strain, as described in Chapter 2.5, then expressed as a proportion of the acetylation level for that.

WT=MSY136-40/*dep1Δ*=JN4/*pho23Δ*=JN6

A similar analysis was also carried out after induction of osmotic stress via 1.2M sorbitol for 30 mins (Figure 11). These stressing conditions were selected as the conditions under which the *rpd3Δ* strain had shown a transcriptional defect when optimising stressing conditions for northern blot analysis (Figure 8). The results are similar to those obtained from analysis after NaCl-induced osmotic stress. WT undergoes increases in acetylation at H3K9 at both gene loci tested (*CTT1* and *HSP12*) after osmotic stressing (Figure 11). Increases in acetylation are also observed at position H4K8, but markedly reduced. This is consistent with the data shown in Figure 9, increasing confidence in the conclusion that acetylation levels do increase at stress-responsive loci after osmotic stress. Again the *rpd3Δ* strains show a different pattern of acetylation at H3K9 in the WT, although this time *dep1Δ* shows decreases in acetylation after osmotic stress, whilst *pho23Δ* shows increases, but to a reduced extent compared to WT. These data are consistent with the conclusions drawn from Figures 9 and 10, that acetylation increases after osmotic stress, and that this is compromised in *rpd3Δ* strains, which are also defective in the transcriptional response to osmostress.

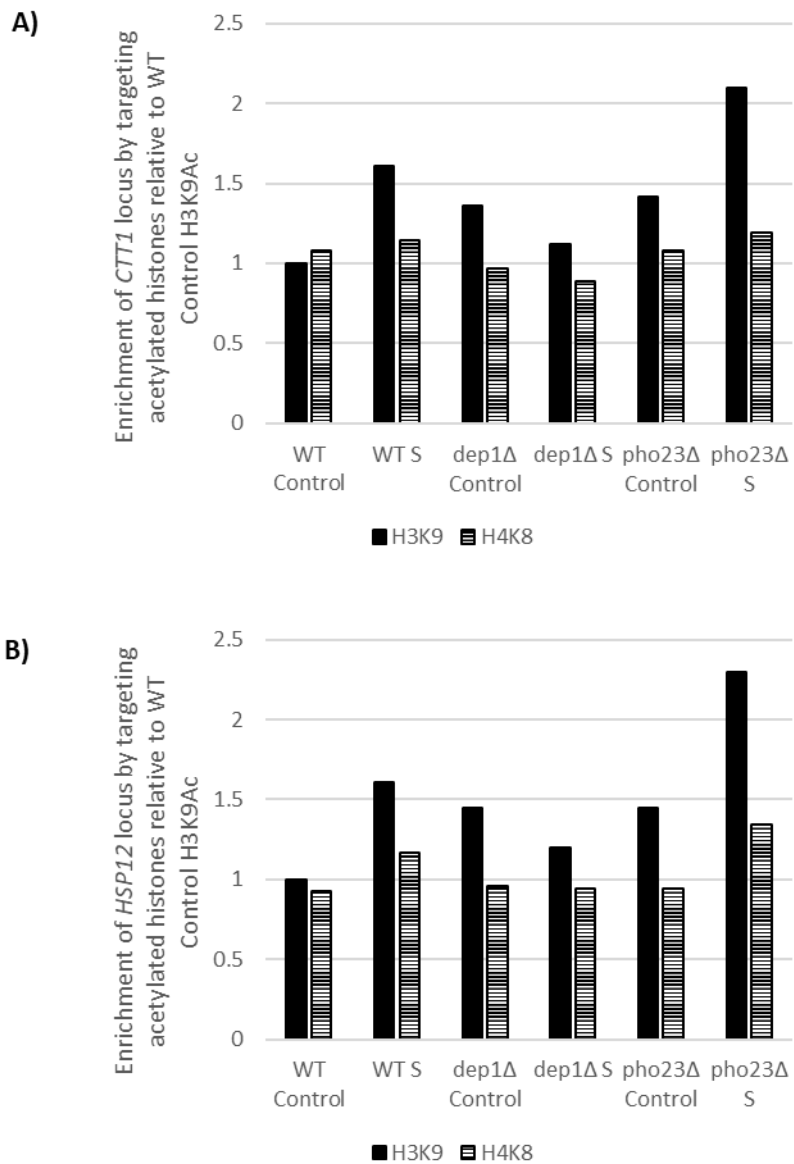


Figure 11 – ChIP-qPCR analysis of changes in histone acetylation after sorbitol-induced osmotic stress in WT and *rpd3Δ* mutants.

Enrichment via targeting H3K9Ac and H4K8Ac of stress-responsive loci *CTT1* (A) and *HSP12* (B) in WT, *dep1Δ*, *pho23Δ* strains before (Control) and after exposure to 1.2M sorbitol for 30 mins (S). Comparative Concentration readings produced by Rotorgene Q software normalised by division against total H3 for that locus and strain, as described in Chapter 2.5, then expressed as a proportion of the normalised acetylation level for H3K9 in the untreated WT.

WT=MSY136-40/*dep1Δ*=JN4/*pho23Δ*=JN6

4.2 *rpd3Δ* strains show general decrease in acetylation after osmotic stress, whilst *rpd3SΔ* strains show a heightened level of acetylation

The same analysis as discussed in 4.1 was also carried out to analyse acetylation in *rpd3Δ* and *rpd3SΔ* strains (*rco1Δ* was selected for this analysis) during the osmotic stress response. The same stressing conditions were used, with WT, *rpd3Δ* strains and *rco1Δ* strains exposed to 0.6M NaCl for 60 mins (Figure 12), and 1.2M sorbitol for 30 mins (Figures 13 and 14). Stemming from my hypothesis that the Rpd3L complex is required for transcriptional induction, it was hypothesised that *rpd3Δ* strains would be defective, but *rpd3SΔ* strains uncompromised in acetylation at stress-responsive loci after osmotic stress. The data in Figures 12 and 13 are consistent with this hypothesis, with *rco1Δ* showing an increase in acetylation at H3K9 after osmotic stress at all genomic loci analysed, and under both osmotic stressing conditions (0.6M NaCl for 60 min and 1.2M sorbitol for 30 mins) (Figures 12 and 13). *rco1Δ* actually shows larger increases in H3K9 acetylation at these positions than WT, which is perhaps unsurprising given it lacks an endogenous deacetylase complex. However, if Rpd3S was mechanistically required for the acetylation process, this increase in acetylation would not be expected to occur. *rpd3Δ* shows a decrease in acetylation at H3K9 at all loci after 1.2M sorbitol-induced osmotic stress, and at *CTT1* after 0.6M NaCl induced osmotic stress (a genomic locus at which the *rpd3Δ* strain was shown to be defective in osmostress-induced transcription in Chapter 3. With *rpd3Δ* strains lacking a potent endogenous deacetylase complex, a decreased level of acetylation is unlikely to be a by-product of generalised changes in acetylation in this strain. Thus, these results are highly suggestive of a mechanistic role for *RPD3* in facilitating acetylation during the osmotic stress response. Again, H3K8

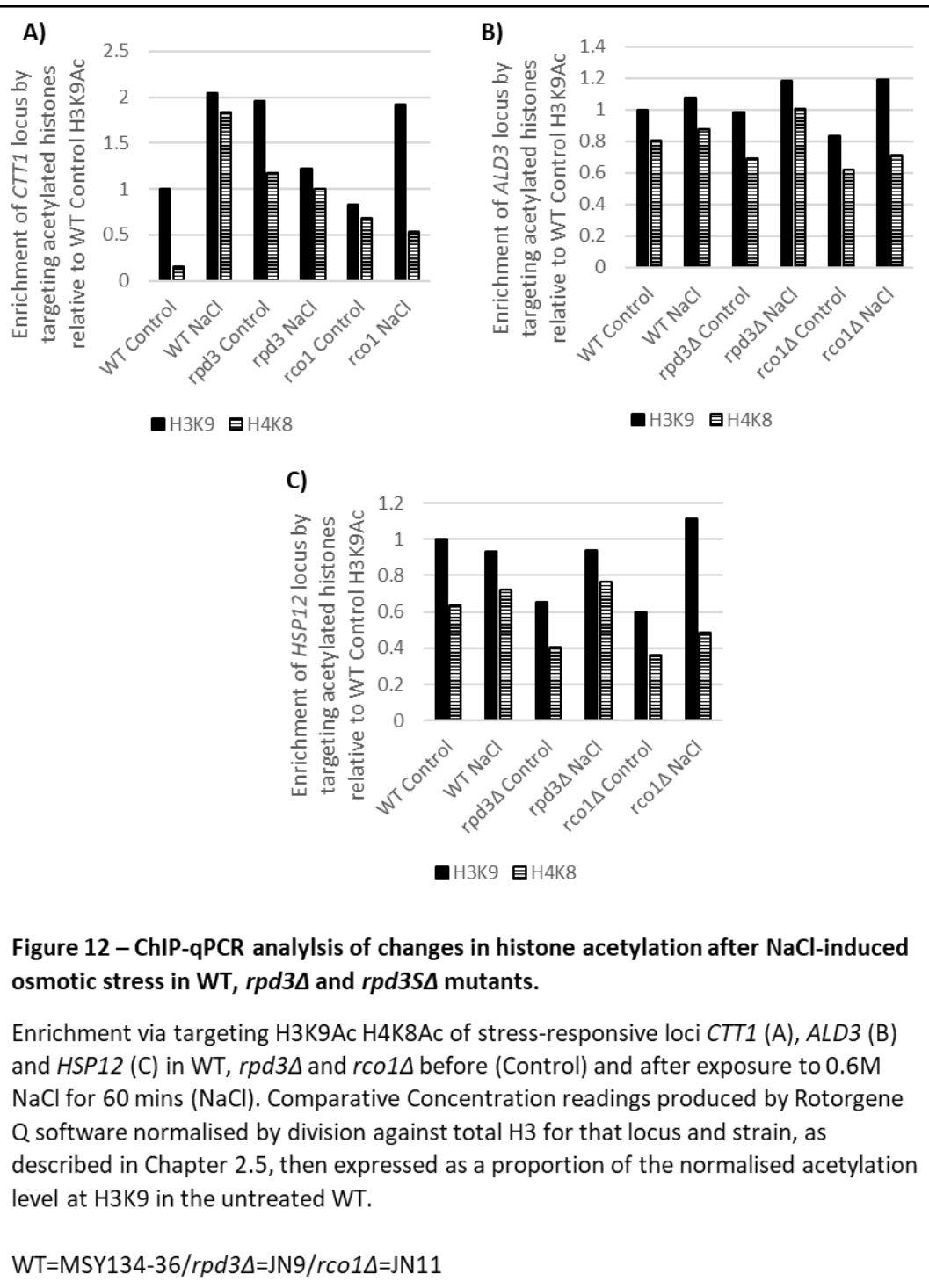


Figure 12 – CHIP-qPCR analysis of changes in histone acetylation after NaCl-induced osmotic stress in WT, *rpd3*Δ and *rpd3*Δ mutants.

Enrichment via targeting H3K9Ac H4K8Ac of stress-responsive loci *CTT1* (A), *ALD3* (B) and *HSP12* (C) in WT, *rpd3*Δ and *rco1*Δ before (Control) and after exposure to 0.6M NaCl for 60 mins (NaCl). Comparative Concentration readings produced by Rotorgene Q software normalised by division against total H3 for that locus and strain, as described in Chapter 2.5, then expressed as a proportion of the normalised acetylation level at H3K9 in the untreated WT.

WT=MSY134-36/*rpd3*Δ=JN9/*rco1*Δ=JN11

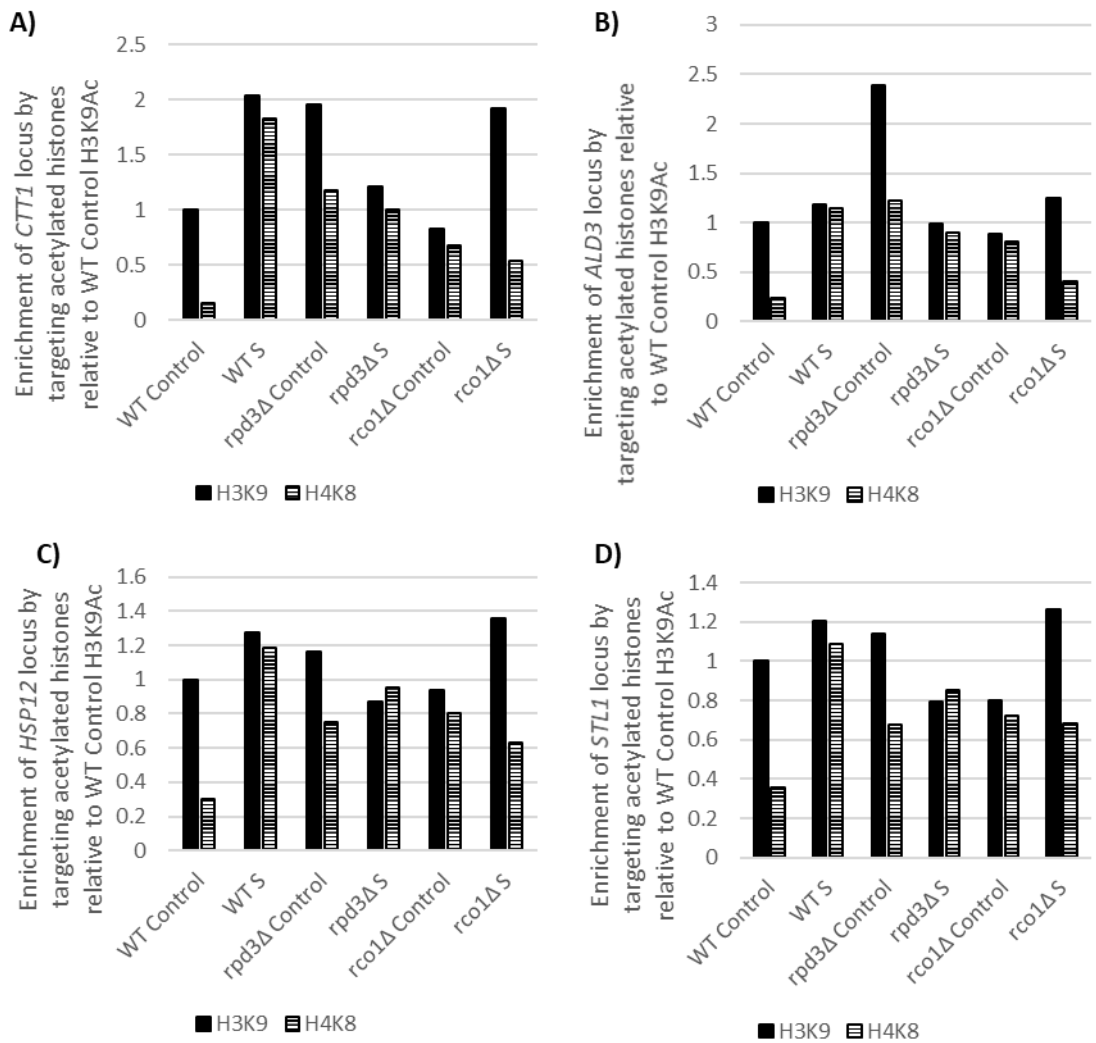


Figure 13 – ChIP-qPCR analysis of changes in histone acetylation after sorbitol-induced osmotic stress in WT, *rpd3Δ* and *rpd35Δ* mutants.

Enrichment via targeting H3K9Ac and H4K8Ac of stress-responsive loci *CTT1* (A), *ALD3* (B), *HSP12* (C) and *STL1* (D) in WT, *rpd3Δ* and *rco1Δ* before (Control) and after exposure to 1.2M sorbitol for 30 mins (S). Comparative Concentration readings produced by Rotorgene Q software normalised by division against total H3 for that locus and strain, as described in Chapter 2.5, then expressed as a proportion of the normalised acetylation level at H3K9 in the untreated WT.

WT=MSY134-36/*rpd3Δ*=JN9/*rco1Δ*=JN11

shows more variation in changes in most strains tested, although in these repeats the WT shows more consistency in acetylation increases at H4K8 than it does at H3K9 (Figures 12 and 13). Two notable trends in H4K8 from these data a strong increase in acetylation at all 4 gene loci analysed in the WT after 1.2M sorbitol-induced osmotic stress (Figure 13), and a consistent decrease in acetylation level under these stressing conditions in *rco1Δ*. These patterns are not consistent with the data shown in Figure 12, in which H4K8 showed little change in the WT after treatment with 1.2M sorbitol. However, if these observations were shown to be reproducible in further repeats, it would be indicative of a defect in acetylation in the *rco1Δ* strain at this position. These data are also more suggestive of a consistent increase in H4K8 acetylation during the osmotic stress response than those presented in Figures 9 and 11.

The effect of 1.2M sorbitol-induced osmotic stress on total H3 occupancy was also analysed in WT, *rpd3Δ*, and *rco1Δ* strains, with total H3 data normalised against input chromatin as described in Chapter 2.5. A distinct decrease in total H3 occupancy at *CTT1* is observed in the WT, which is also present (albeit to a reduced extent) in the *rco1Δ* strain (Figure 14). *rpd3Δ*, meanwhile, shows a distinct increase in total H3 occupancy (Figure 14). This data supports the experimental hypothesis that *RPD3*-dependent loss of histones occurs during osmotic stress, and that this is unaffected by loss of the Rpd3S complex (which is hypothesised to be not required for the transcriptional responses to osmotic stress).

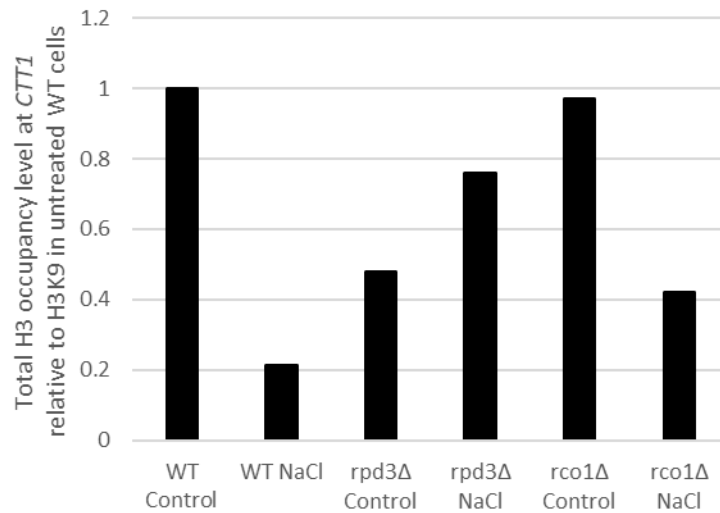


Figure 14 – ChIP-qPCR analysis of changes in H3 occupancy after sorbitol-induced osmotic stress in WT, *rpd3Δ* and *rpd3Δ* mutants.

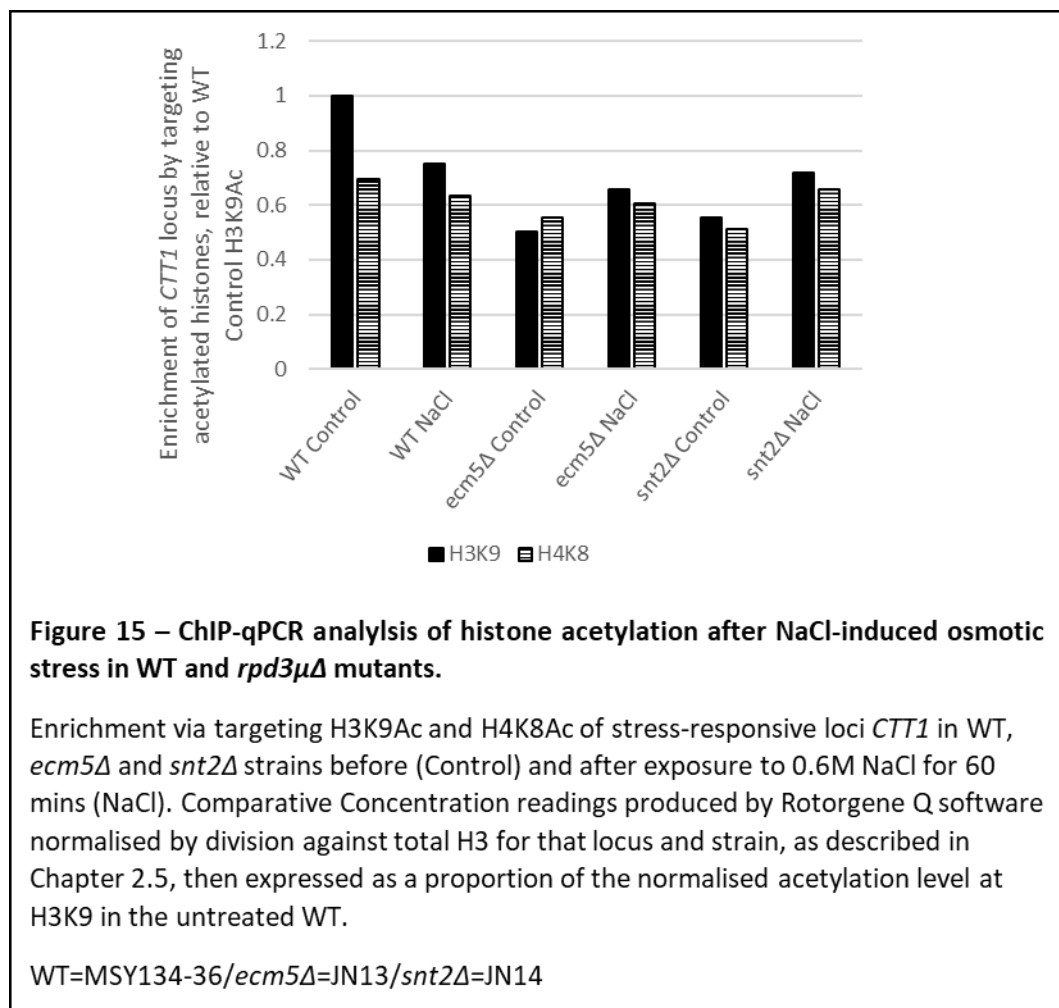
Total H3 levels at stress-responsive loci *CTT1* in WT, *dep1Δ*, *pho23Δ* strains before (Control) and after exposure to 1.2M sorbitol for 30 mins (S). Comparative Concentration readings were produced by Rotorgene Q software were normalised by division against Input Chromatin for the same locus and strain, as described in Chapter 2.5, then expressed as a proportion of the acetylation level for that. All strains are mating type a, with MSY134-36 used as WT.

WT=MSY134-36/*rpd3Δ*=JN9/*rco1Δ*=JN11

4.3 *rpd3μΔ* strains show acetylation at H3K9 and H4K8 during the osmotic stress response

The same analysis was also carried out to analyse acetylation in *rpd3μΔ* strains *ecm5Δ* and *snt2Δ*, generated by PCR-mediated gene deletion as described in Chapter 2.5. It was difficult to generate hypotheses about the behaviour of *rpd3μΔ* strains in the osmotic stress response due to a paucity of literature analysis of the complex, and the fact that the two subunits *ECM5* and *SNT2* have been observed to have opposing effects upon gene induction in response to oxidative stress (Baker et al., 2013). The results of ChIP-qPCR analysis identified a small increase in acetylation at both H3K9 and H4K8 in *ecm5Δ* and *snt2Δ* strains at the *CTT1* gene locus (Figure 15) after 0.6M NaCl-induced osmotic

stress. In contrast, the WT exhibited a decrease in acetylation after osmotic stressing (Figure 15) at this locus at both H3K9 and H4K8 (although the decrease in acetylation at H4K8 is small). This result is not consistent with other data presented in this thesis (Figures 9, 10, 12 and 13) which all found a strong increase in acetylation at *CTT1*. Thus, it may be that the data shown in Figure 15 is erroneous, and not reflective of acetylation patterns during osmotic stressing. Such error could have potentially been introduced by human pipetting error during the lengthy wash steps of the immunoprecipitation, or if the aliquot of α -H3K9Ac antibody used for certain samples (e.g. NaCl-treated WT) had been unknowingly damaged by previous freeze-thaw cycles. Antibodies were routinely stored at -80°C in $5\mu\text{L}$ aliquots in the laboratory, meaning it was not possible to use the same aliquot for all immunoprecipitations.



4.4 Summary and discussion of ChIP-qPCR analysis

Overall, a conclusion can be drawn that acetylation at both H3K9 and H4K8 increases during the osmotic stress response in *S. cerevisiae*. The analysis of WT and *rpd3Δ* strains in response to 0.6M NaCl-induced osmotic stress displayed in Figures 9 and 10 provide the most consistent data with respect to H3K9 acetylation levels. All strains show a similar pattern of change in acetylation at H3K9 after osmotic stress (Figure 9), and except for *pho23Δ* at the *STL1* locus, a consistent change in H3 occupancy as well (Figure 10). The data for these strains after treatment with 1.2M sorbitol is also internally consistent, finding an increase in acetylation at H3K9 in the WT at *CTT1* and *HSP12*, which is lessened in *rpd3Δ* strains (Figure 11). Overall, the data in Figures 9, 10, and 11 appear robust and provide evidence to support the conclusion that acetylation alongside histone loss occurs at H3K9 during the osmotic stress response, and that this is dependent upon the Rpd3L complex.

Data obtained for *rpd3Δ*, *rpd35Δ* and *rpd3Δ* strains also offers evidence to support the hypotheses that *rpd3Δ* strains are required for acetylation and transcriptional induction, but *Rpd35* and *Rpd3μ* complexes are not. However, although these data largely support the experimental hypotheses, caution must be exercised in drawing conclusions due to irregularities in the observations for WT strain. The WT is generally found to increase increase in acetylation at H3K9 after osmotic stress induced by both 0.6M NaCl and 1.2M sorbitol (Figures 12 and 13), but the effect is often small, whilst a slight *decrease* is observed in acetylation at H3K9 at the *HSP12* gene locus in the WT in response to 0.6M NaCl (Figure 12). This result is also found in Figure 15, analysing WT and *rpd3μΔ* strains at the *CTT1* locus. The lack of corroboration between these repeats

and the data shown in Figures 9 to 11 raises questions of reproducibility of the data, and thus limits the strength of the conclusions that can be drawn from the data in Figures 9 to 11. However, it is worth mentioning that this could be simply down to a lack of WT transcriptional competency in these repeats. Aside from the WT strains, Figures 12 and 13 display data largely in keeping with what was expected, with *rco1Δ* showing distinct increases in acetylation at H3K9 after osmotic stress, whilst *rpd3Δ* mostly exhibits decreases. The histone occupancy data also follows this trend, with *rco1Δ* showing a distinct decrease in total H3 at *CTT1* after osmotic stress, whilst *rpd3Δ* shows an increase. Thus, it could simply be that the WT strains used in this report were not fully competent with regards to the osmotic stress response, resulting in the unexpected results for WT strains in Figures 12 and 13.

A general conclusion can be drawn that the data supports the notion that Rpd3L-dependent histone acetylation and nucleosome loss occurs at upregulated loci during the osmotic stress response. Nevertheless, lack of consistency *between repeats* in the data obtained with only tentative conclusions can be drawn, with limited confidence in the results. It must also be noted that the lack of repeats for the same immunoprecipitation means that statistical analysis was not possible for this data, and thus conclusions cannot be backed up by demonstrable statistical significance. This stemmed from the delays encountered in the Northern blot analysis, which meant that further repeats could not be carried out within the timeframe. An immediate priority for further work would be to carry out more repeats of these analyses, rectify the lack of consistency observed in WT responses in further repeats, and carry out statistical analysis on the data to identify if differences in acetylation are statistically significant.

Chapter 5 – General discussion and priorities for further work

5.1 *rpd3Δ* strains display a general defect in transcriptional responses to osmotic stress

The main underlying hypothesis of this project was that *rpd3Δ* strains would display a defect in the transcriptional responses to osmotic stress, whilst *rpd35Δ* strains would not. In line with this observation, a reduced expression at *CTT1* and *GRE2* is observed in *rpd3Δ* strains after induction of osmotic stress by both 0.6M NaCl and 1.2M sorbitol (Figures 5 and 6), compared to WT strains exposed for the same length of time. The observation of a transcriptional defect in *rpd3Δ* strains in response to two separate osmotic stressing reagents increases confidence that the defect observed is related to the osmotic stress response. The nature of the defect in the transcriptional response is worthy of further investigation. The data presented in the time course experiments in Figure 8 shows expression of *CTT1* in the *rpd3Δ* strain 60-90 minutes after exposure to 1.2M Sorbitol, compared to 30 minutes after exposure to the same stressing condition in the WT strain. This raises the possibility that the *rpd3Δ* is transcriptionally competent, but with a slower response time than the WT strain. This data conflicts with previous findings in (Alejandro-Osario et al., 2009), which measured expression of induced environmental stress response (iESR) genes after exposure to heat shock, oxidative and NaCl-induced osmotic stress. Under all three stressing conditions, *rpd3Δ* strains were found to exhibit transcription of iESR genes at the same time as WT strains, but to a lesser extent (Alejandro-Osario et al., 2009). Moreover, an analysis of *CTT1* expression in *rpd3Δ* strains in (Ruiz-Roig et al., 2010) shows *CTT1* expression peaking at 15 minutes (though also at a lower level than in the WT) and then

decreasing by 30 minutes (Ruiz-Roig et al., 2010). It is difficult to reconcile the findings of the time course experiment in Figure 8 with these previous observations in the literature given the limitations of the northern blotting data in this thesis. The technical challenges discussed in Chapter 3 also affected the time course experiments, limiting the conclusions that can be drawn. Further blots to produce more robust information on the temporal regulation of transcription in WT and *rpd3Δ* strains would be desirable to help resolve this conflict.

The transcriptional defect in *rpd3LΔ* strains is not apparent in *rpd3SΔ* strains (Figure 7), though as discussed in Chapter 3.2 less reliable data is obtained for this complex.

These observations are consistent both with previous unpublished work in our group, and with literature observations for other stresses (Loewith et al., 2001, Alejandro-Osario et al., 2009, Ruiz-Roig et al., 2010). It is also consistent with several observed features of the osmotic stress response and *RPD3* recruitment. *Rpd3L* is found to localise to the promoters of genes, whilst *Rpd3S* is recruited to gene bodies instead (Alejandro-Osario et al., 2009). More recently, it has been found that acetylation clustering towards the promoter is important in inducing transcription during the osmotic stress response (Magraner-Pardo et al., 2014), offering an explanation as to why a chromatin modifier localising to this region will have more of an impact on transcription. Additionally, it has been proposed in the literature that *Hog1* may recruit *RPD3* to gene bodies via the *Rpd3L* complex (Saito and Posas, 2012).

Overall the data presented support the conclusion that *Rpd3L* playing a role in transcriptional responses to osmotic stress. This observation is consistent with

literature observations regarding both its role in other stresses, and molecular details of the osmotic stress response.

5.2 Histone acetylation and nucleosome loss is observed during the osmotic stress response, and a defect is observed in *rpd3 Δ* strains

The data in this research find a general increase in acetylation at H3K9 and H4K8, alongside nucleosome loss, in WT strains after induction of osmotic stress by 0.6M NaCl and 1.2M Sorbitol (Figures 9 to 15). This finding is consistent with literature observations (Magraner Pardo et al., 2014) as well as previous work in the Schroder laboratory (unpublished). These features are generally found to be missing or reduced relative to WT in both *rpd3 Δ* and *rpd3L Δ* strains (*dep1 Δ* and *pho23 Δ*) (Figures 9 to 14). Both *rpd3S Δ* strains and *rpd3 μ* strains show similar or higher increases in acetylation than WT (Figures 12, 13 and 15), though this may be due to a lack of transcriptional competency in the WT strains during these repeats. The decreased acetylation observed in *rpd3 Δ* and *rpd3L Δ* strains is noteworthy as it contradicts what would be expected from loss of an endogenous histone deacetylase (i.e. an increase in acetylation), suggesting a mechanistic link between *RPD3* and histone acetylation in this process. This is further suggested by the correlation observed between the strains displaying a defect in transcriptional responses, and the strains displaying reduced acetylation or deacetylation during the osmotic stress response (namely *rpd3 Δ* and *rpd3L Δ* strains).

H3K9 and H4K8 show different patterns of acetylation in these data. In general, the changes observed at position H3K9 are larger than those at H4K8 (Although it must be noted that the WT strain in Figure 13 provides an exception to this, with larger

increases seen at H4K8, and relatively little change at H3K9). Based on observations in the literature, the acetylation levels at H3K9 is proposed to have more significance to the transcriptional responses to osmotic stress. This position has been described in the literature as showing the greatest change in acetylation in response to osmotic stress, and also showing the greatest correlation with Pol II occupancy and thus gene expression (Magraner-Pardo et al., 2014). This paper also offers an explanation as to how H3K9 may be mechanistically linked to the yeast osmotic stress response in a way that H4K8 is not. The SAGA complex is recruited to osmostress-upregulated gene loci, and contains the Gcn5 subunit which specifically acetylates positions H3K9 and H3K14 (Magraner-Pardo et al., 2014). As mentioned previously, if acetylation at H3K9 is integral to the osmotic stress response, whilst acetylation at H4K8 is not, then it is may be that H3K9Ac levels may be more tightly regulated during this process, whilst H4K8Ac may be subject to higher levels of fluctuation. Thus the results for H3K9Ac are taken to be more indicative of biological phenomena than those for H4K8Ac.

Overall, our ChIP-qPCR data agree with recent literature findings (Magraner-Pardo et al., 2014), whilst disagreeing with those made earlier (De Nadal et al., 2004). The most obvious explanation seems to be a difference in normalisation methods, with nucleosome loss resulting in a reduced acetylation signal being observed if total histone occupancy is not accounted for. (Magraner-Pardo et al., 2014) found that their findings agreed with (De Nadal et al., 2004) if normalised against an external genomic locus, but differed when considering nucleosome occupancy. Thus, it seems reasonable to hypothesise that nucleosome loss is occurring alongside acetylation at the remaining histones. This would also be consistent with findings in the literature

that nucleosome-depleted regions are found near the start of actively transcribed genes (Lee et al., 2004, Li et al., 2007).

5.3 Summary of data and potential hypotheses

Overall, two trends can be observed which are consistent with previous findings.

Firstly, *RPD3* strains do display a general defect in transcriptional responses to osmotic stress induced by multiple osmotic stressing reagents (0.6M NaCl and 1.2M sorbitol). Secondly, site-specific changes in acetylation and histone loss do seem to occur in WT strains at up-regulated gene loci, and these features are consistently reduced or reversed in *RPD3* strains under multiple osmotic stressing reagents (0.6M NaCl and 1.2M Sorbitol).

RPD3 is well known to be required for the osmotic stress response, and the prevailing view in the literature that the Rpd3L complex is predominant in transcriptional responses to stress in *S. cerevisiae* (Alejandro-Osario et al., 2009, Ruiz-Roig et al., 2010, Saito and Posas, 2012). Thus the data presented in this thesis correlates with the literature in this regard. It is also noteworthy that the deacetylase activity is required for transcriptional induction (De Nadal et al., 2004, Zapater et al., 2007, Alejandro-Osario et al., 2009). However, both these data and more recent literature observations have found an increase in acetylation at upregulated gene loci during the osmotic stress response (Magraner-Pardo et al., 2014). This acetylation seems to be accompanied by histone loss and to show site-specific, with differences in acetylation found at H3K9 and H4K8 in these data and in the literature (Magraner-Pardo et al., 2014).

Thus, taking into account both data presented in this report and previous literature findings, a model can be hypothesised whereby *RPD3*, functioning through the Rpd3L complex, catalyses deacetylation at stress-responsive loci, which indirectly induces transcription through acting as a recruitment signal for other chromatin modifying proteins. The overall process would be hypothesised to then involve site specific acetylation by unknown factors (perhaps the SAGA complex) recruited in an *RPD3*-dependent manner. This would be difficult to test directly, and would require consideration of temporal information and site-specific differences in acetylation state. For example, if two time points were selected, an initial *RPD3*-dependent decrease in acetylation catalysed might be observed, followed by a later increase (dependent on unknown factors) and then followed by transcriptional initiation. Equally, site-specific deacetylation may occur concurrently with an increase in acetylation at other residues, giving an overall increase in acetylation. It is also hypothesised that nucleosome depletion near the transcriptional start site is involved in this process, both based on my data and previous observations of the osmotic stress response (Magraner-Pardo et al., 2014).

5.4 Priorities for further work in this area

As discussed the immediate priority would be to identify and resolve the reasons behind the challenges encountered with northern blotting, so that further repeats of the quality seen in Figure 5 can be carried out. The first priority is to provide robust evidence regarding which *RPD3* complexes were, and just as crucially which were *not*, required for transcriptional induction. To establish this conclusively requires several repeats of the quality seen in Figure 5 analysing transcriptional responses in strains

carrying deletions in all each of the three *RPD3* complexes. Further analysis of the temporal nature of transcriptional responses in different strains via time course analysis would be desirable to identify whether *rpd3Δ* strains show *reduced* or *delayed* expression of stress-responsive genes. This work should then be extended to analyse time courses of transcription in *rpd3LΔ* strains and *rpd3SΔ* strains in the same fashion. The next priority would be to carry out further repeats of the CHIP-qPCR data, to identify which discrepancies represent meaningful biological variation, and estimate the error inherent in the measurements. However, the CHIP-qPCR data would also be inherently made more informative if it could be correlated with robust northern blotting data showing the transcriptional responses of *rpd3SΔ* and *rpd3μΔ* strains to osmotic stress.

Once these technical issues were resolved, it would be useful to analyse acetylation at other histone residues, particularly those known to be most affected by *RPD3* histone deacetylase activity, or strongly involved with transcriptional activation. For example acetylation at H3K14 has also been found to increase during the osmotic stress response, and acetylation at this site is catalysed by SAGA as with H3K9 (Magraner-Pardo et al., 2014). If H3K14 shows similar patterns of acetylation to H3K9, but H4K8 continues to differ, it would be consistent with *RPD3* playing a role mediating site-specific acetylation via recruitment of specific chromatin modifiers.

It would also be useful to examine acetylation levels at different points in the transcriptional response. If deacetylation was found to occur quickly (5-10 mins) and was then followed by acetylation and then transcription this would be consistent with

the model proposed of *RPD3* deacetylating to act as a recruitment signal for downstream effectors.

With this additional information, a more in-depth and detailed picture would be available of the mechanisms by which *RPD3* mediates the transcriptional responses to osmotic stress. This may also be informative with regards to the dynamics of histone modifications more generally and how they regulate transcription.

Chapter 6 – Bibliography

- Alejandro-Osorio, A.L., Huebert, D.J., Porcaro, D.T., Sonntag, M.E., Nillasithanukroh, S., Will, J.L., and Gasch, A.P. (2009). The histone deacetylase Rpd3p is required for transient changes in genomic expression in response to stress. *Genome Biol.* 10, R57.
- Alepuz, P.M., de Nadal, E., Zapater, M., Ammerer, G., and Posas, F. (2003). Osmostress-induced transcription by Hot1 depends on a Hog1-mediated recruitment of the RNA Pol II. *EMBO J* 22, 2433–2442.
- Alepuz, P.M., Jovanovic, A., Reiser, V., and Ammerer, G. (2001). Stress-Induced MAP Kinase Hog1 Is Part of Transcription Activation Complexes. *Molecular Cell* 7, 767–777.
- Baker, L.A., Ueberheide, B.M., Dewell, S., Chait, B.T., Zheng, D., and Allis, C.D. (2013). The Yeast Snt2 Protein Coordinates the Transcriptional Response to Hydrogen Peroxide-Mediated Oxidative Stress. *Mol Cell Biol* 33, 3735–3748.
- Baker, L.A., Ueberheide, B.M., Dewell, S., Chait, B.T., Zheng, D., and Allis, C.D. (2013). The yeast Snt2 protein coordinates the transcriptional response to hydrogen peroxide-mediated oxidative stress. *Mol. Cell. Biol.* 33, 3735–3748.
- Bannister, A.J., and Kouzarides, T. (2011). Regulation of chromatin by histone modifications. *Cell Res* 21, 381–395
- Baudin, A., Ozier-Kalogeropoulos, O., Denouel, A., Lacroute, F., and Cullin, C. (1993a). A simple and efficient method for direct gene deletion in *Saccharomyces cerevisiae*. *Nucleic Acids Res* 21, 3329–3330.
- Berger, S.L. (2007). The complex language of chromatin regulation during transcription. *Nature* 447, 407–412
- Carrozza, M.J., Li, B., Florens, L., Suganuma, T., Swanson, S.K., Lee, K.K., Shia, W.-J., Anderson, S., Yates, J., Washburn, M.P., et al. (2005). Histone H3 Methylation by Set2 Directs Deacetylation of Coding Regions by Rpd3S to Suppress Spurious Intragenic Transcription. *Cell* 123, 581–592.
- Chen, D.C., Yang, B.C., and Kuo, T.T. (1992). One-step transformation of yeast in stationary phase. *Current genetics* 21, 83-84.

- De Nadal, E., Zapater, M., Alepuz, P.M., Sumoy, L., Mas, G., and Posas, F. (2004). The MAPK HOG1 recruits *RPD3* histone deacetylase to activate osmoresponsive genes. *Nature* 427, 370–374.
- Deckert, J., and Struhl, K. (2002). Targeted recruitment of *RPD3* histone deacetylase represses transcription by inhibiting recruitment of Swi/Snf, SAGA, and TATA binding protein. *Mol. Cell. Biol.* 22, 6458–6470.
- Dolz-Edo, L., Rienzo, A., Poveda-Huertes, D., Pascual-Ahuir, A., and Proft, M. (2013). Deciphering Dynamic Dose Responses of Natural Promoters and Single cis Elements upon Osmotic and Oxidative Stress in Yeast. *Mol Cell Biol* 33, 2228–2240.
- Fussner, E., Ching, R.W., and Bazett-Jones, D.P. (2011). Living without 30 nm chromatin fibers. *Trends in Biochemical Sciences* 36, 1–6.
- Gajan, A., Barnes, V.L., Liu, M., Saha, N., and Pile, L.A. (2016). The histone demethylase dKDM5/LID interacts with the SIN3 histone deacetylase complex and shares functional similarities with SIN3. *Epigenetics Chromatin* 9.
- Guarente, L., and Kenyon, C. (2000). Genetic pathways that regulate ageing in model organisms. *Nature* 408, 255–262.
- J. Sambrook, E. F. Fritsch, and T. Maniatis, Commonly used techniques in molecular cloning. Measurement of radioactivity in nucleic acids in *Molecular Cloning. A Laboratory Manual*, Vol. 3, 2nd ed., Cold Spring Harbor Laboratory Press, Cold Spring Harbor, 1989, pp.E.18 - E.19.
- Josling, G.A., Selvarajah, S.A., Petter, M., and Duffy, M.F. (2012). The Role of Bromodomain Proteins in Regulating Gene Expression. *Genes (Basel)* 3, 320–343.
- Kadosh, D., and Struhl, K. (1997). Repression by Ume6 Involves Recruitment of a Complex Containing Sin3 Corepressor and *RPD3* Histone Deacetylase to Target Promoters. *Cell* 89, 365–371.
- Kadosh, D., and Struhl, K. (1998). Histone deacetylase activity of *RPD3* is important for transcriptional repression in vivo. *Genes Dev.* 12, 797–805.

- Kane, S.M., and Roth, R. (1974). Carbohydrate Metabolism During Ascospore Development in Yeast. *J Bacteriol* 118, 8–14.
- Keogh, M.-C., Kurdistani, S.K., Morris, S.A., Ahn, S.H., Podolny, V., Collins, S.R., Schuldiner, M., Chin, K., Punna, T., Thompson, N.J., et al. (2005). Cotranscriptional Set2 Methylation of Histone H3 Lysine 36 Recruits a Repressive *RPD3* Complex. *Cell* 123, 593–605.
- Koressaar T, Remm M (2007) Enhancements and modifications of primer design program Primer3 *Bioinformatics* 23(10):1289-91
- Kugler, K.G., Jandric, Z., Beyer, R., Klopf, E., Glaser, W., Lemmens, M., Shams, M., Mayer, K., Adam, G., and Schüller, C. (2016). Ribosome quality control is a central protection mechanism for yeast exposed to deoxynivalenol and trichothecin. *BMC Genomics* 17.
- Kurdistani, S.K., Tavazoie, S., and Grunstein, M. (2004). Mapping Global Histone Acetylation Patterns to Gene Expression. *Cell* 117, 721–733.
- Lee, C.-K., Shibata, Y., Rao, B., Strahl, B.D., and Lieb, J.D. (2004). Evidence for nucleosome depletion at active regulatory regions genome-wide. *Nat Genet* 36, 900–905.
- Li, B., Carey, M., and Workman, J.L. (2007). The Role of Chromatin during Transcription. *Cell* 128, 707–719.
- Loewith, R., Smith, J.S., Meijer, M., Williams, T.J., Bachman, N., Boeke, J.D., and Young, D. (2001). Pho23 Is Associated with the *RPD3* Histone Deacetylase and Is Required for Its Normal Function in Regulation of Gene Expression and Silencing in *Saccharomyces cerevisiae*. *J. Biol. Chem.* 276, 24068–24074.
- Magraner-Pardo, L., Pelechano, V., Coloma, M.D., and Tordera, V. (2014). Dynamic remodeling of histone modifications in response to osmotic stress in *Saccharomyces cerevisiae*. *BMC Genomics* 15.

Mas, G., de Nadal, E., Dechant, R., de la Concepción, M.L.R., Logie, C., Jimeno-González, S., Chávez, S., Ammerer, G., and Posas, F. (2009). Recruitment of a chromatin remodelling complex by the HOG1 MAP kinase to stress genes. *EMBO J* 28, 326–336.

McDaniel, S.L., and Strahl, B.D. (2013). Stress-Free with Rpd3: a Unique Chromatin Complex Mediates the Response to Oxidative Stress. *Mol Cell Biol* 33, 3726–3727.

Oakes, M.L., Siddiqi, I., French, S.L., Vu, L., Sato, M., Aris, J.P., Beyer, A.L., and Nomura, M. (2006). Role of Histone Deacetylase *RPD3* in Regulating rRNA Gene Transcription and Nucleolar Structure in Yeast. *Mol Cell Biol* 26, 3889–3901.

Pazin, M.J., and Kadonaga, J.T. (1997). What's Up and Down with Histone Deacetylation and Transcription? *Cell* 89, 325–328.

Pennisi, E. (1997). Opening the Way to Gene Activity. *Science* 275, 155–157.

Pokholok, D.K., Harbison, C.T., Levine, S., Cole, M., Hannett, N.M., Lee, T.I., Bell, G.W., Walker, K., Rolfe, P.A., Herbolsheimer, E., et al. (2005). Genome-wide Map of Nucleosome Acetylation and Methylation in Yeast. *Cell* 122, 517–527.

Raffaello, T., Keriö, S., and Asiegbu, F.O. (2012). Role of the HaHOG1 MAP Kinase in Response of the Conifer Root and But Rot Pathogen (*Heterobasidion annosum*) to Osmotic and Oxidative Stress. *PLOS ONE* 7, e31186.

Rando, O.J., and Chang, H.Y. (2009). Genome-Wide Views of Chromatin Structure. *Annu Rev Biochem* 78, 245–271.

Ren, B., Robert, F., Wyrick, J.J., Aparicio, O., Jennings, E.G., Simon, I., Zeitlinger, J., Schreiber, J., Hannett, N., Kanin, E., et al. (2000). Genome-Wide Location and Function of DNA Binding Proteins. *Science* 290, 2306–2309.

Ruiz-Roig, C., Viéitez, C., Posas, F., and De Nadal, E. (2010). The Rpd3L HDAC complex is essential for the heat stress response in yeast. *Molecular Microbiology* 76, 1049–1062.

Rundlett, S.E., Carmen, A.A., Kobayashi, R., Bavykin, S., Turner, B.M., and Grunstein, M. (1996). HDA1 and RPD3 are members of distinct yeast histone deacetylase complexes that regulate silencing and transcription. *Proc Natl Acad Sci U S A* 93, 14503–14508.

- Saito, H., and Posas, F. (2012). Response to Hyperosmotic Stress. *Genetics* 192, 289–318.
- Schröder, M., Chang, J.S., and Kaufman, R.J. (2000). The unfolded protein response represses nitrogen-starvation induced developmental differentiation in yeast. *Genes Dev* 14, 2962–2975.
- Schröder, M., Clark, R., Liu, C.Y., and Kaufman, R.J. (2004). The unfolded protein response represses differentiation through the RPD3-SIN3 histone deacetylase. *EMBO J* 23, 2281–2292.
- Sertil, O., Vemula, A., Salmon, S.L., Morse, R.H., and Lowry, C.V. (2007). Direct Role for the *RPD3* Complex in Transcriptional Induction of the Anaerobic DAN/TIR Genes in Yeast. *Mol Cell Biol* 27, 2037–2047.
- Soufi, B., D. Kelstrup, C., Stoehr, G., Fröhlich, F., C. Walther, T., and V. Olsen, J. (2009). Global analysis of the yeast osmotic stress response by quantitative proteomics. *Molecular BioSystems* 5, 1337–1346.
- Sternglanz, R. (1996). Histone acetylation: a gateway to transcriptional activation. *Trends in Biochemical Sciences* 21, 357–358.
- Stuparevic, I., Becker, E., Law, M.J., and Primig, M. (2015). The histone deacetylase Rpd3/Sin3/Ume6 complex represses an acetate-inducible isoform of VTH2 in fermenting budding yeast cells. *FEBS Letters* 589, 924–932.
- Tong, E.H.Y., Guo, J.-J., Xu, S.-X., Mak, K., Chung, S.K., Chung, S.S.M., Huang, A.-L., and Ko, B.C.B. (2009). Inducible Nucleosome Depletion at OREBP-Binding-Sites by Hypertonic Stress. *PLOS ONE* 4, e8435.
- Vidal, M., and Gaber, R.F. (1991). RPD3 encodes a second factor required to achieve maximum positive and negative transcriptional states in *Saccharomyces cerevisiae*. *Mol. Cell. Biol.* 11, 6317–6327.
- Vidal, M., Buckley, A.M., Hilger, F., and Gaber, R.F. (1990). Direct Selection for Mutants with Increased K(+) Transport in *Saccharomyces Cerevisiae*. *Genetics* 125, 313–320.

Yehekely-Hayon, D., Kotler, A., Stark, M., Hashimshony, T., Sagee, S., and Kassir, Y. (2013). The Roles of the Catalytic and Noncatalytic Activities of Rpd3L and Rpd3S in the Regulation of Gene Transcription in Yeast. *PLoS One* 8.

Zapater, M., Sohrmann, M., Peter, M., Posas, F., and de Nadal, E. (2007). Selective requirement for SAGA in HOG1-mediated gene expression depending on the severity of the external osmostress conditions. *Mol. Cell. Biol.* 27, 3900–3910.

Zupkovitz, G., Tischler, J., Posch, M., Sadzak, I., Ramsauer, K., Egger, G., Grausenburger, R., Schweifer, N., Chiocca, S., Decker, T., et al. (2006). Negative and Positive Regulation of Gene Expression by Mouse Histone Deacetylase 1. *Mol Cell Biol* 26, 7913–7928.